Exploring the Forces Contributing to Non-Covalent Bonding by Microwave Spectroscopy and Structural Characterization of Gas-Phase Heterodimers of Protic Acids with Haloethylenes

Helen O. Leung* and Mark D. Marshall*

Department of Chemistry, Amherst College, P.O. Box 5000, Amherst, MA 01002-5000

Address for correspondence: Prof. Helen O. Leung
Department of Chemistry
Amherst College
P.O. Box 5000
Amherst, MA 01002-5000
Telephone: (413) 542-2660
Fax: (413) 542-2735
E-mail: hleung@amherst.edu

*Corresponding authors. Fax: +1-413-542-2735; *e-mail addresses:* hleung@amherst.edu (H.O. Leung), mdmarshall@amherst.edu (M.D. Marshall).

The authors declare no competing financial interest.

Abstract

A detailed comparison of structural parameters obtained via microwave rotational spectroscopy in a systematic study of protic acid-haloethylene heterodimers is used to investigate the forces contributing to intermolecular interactions. Conclusions reached using structural data and chemical intuition are supplemented with information obtained from quantum chemistry calculations to refine the understanding of the various contributions to complex formation. The observed structures, representative of the global minimum on the potential energy surface, are found to reflect a balance between optimal electrostatics and steric requirements, or in other words, how well the two interacting molecules fit together. Structural trends are rationalized in terms of familiar chemical concepts of the electrophilicity or nucleophilicity of interaction sites as modulated by electron withdrawing and electron donating groups along with the geometric requirements for optimal interactions between the two molecules.

1. Introduction

Though much weaker than chemical forces, van der Waals interactions are present in large numbers in a chemical or biological system, making them very significant to a complete description or understanding of these systems. These intermolecular interactions include electrostatic forces due to permanent and induced moments, as well as quantum mechanical interactions (London dispersion forces).[1] They are responsible for many physical and chemical properties of matter, from the condensation of gases and low temperature gas viscosity,[2] to the sticky feet of a gecko,[3] to influencing the structure, and therefore, the reactivity of molecules,[4] and to playing active roles in regulatory functions.[5] A deep understanding of these interactions is therefore critical in advancing chemistry at a fundamental level. The importance and effects of one type of van der Waals bond, the hydrogen bond, are particularly well appreciated; for example, it is central to the properties of liquid water,[1] the secondary and tertiary structures of proteins, and the double helix structure of DNA,[6] to name only a few examples.

These weak intermolecular forces are subtle and are usually masked by the larger effects of the chemical bond. To focus primarily on the contributions of intermolecular interactions, we study systems that owe their very existence to these forces – gas phase dimers formed between two molecules (or an atom and a molecule). We are particularly interested in understanding the delicate balance of forces that gives rise to these complexes. Specifically, we wish to explore the roles that electron withdrawing and electron donating functionalities play in modulating intermolecular interactions.

Since the early days of modern organic chemistry and continuing to the present, these functionalities have been recognized to influence both the site of reaction and the identity of the products in chemical processes.[7-8] Indeed, the successful interpretation of the results of

electrophilic aromatic substitution reactions using these concepts has made them a standard topic in introductory organic chemistry courses. Certainly, these effects arise from the stabilization or destabilization of transition states or intermediates for the reaction, but weakly bound complexes in the entrance channel of reactions can also have a profound influence on chemical reaction rates and product distributions.[9-13] It is, therefore, imperative to determine the structure and dynamics of molecular complexes and to characterize the forces that are responsible for their formation.

Lewis bases and protic acids are ideal model systems for our inquiry. Based on a series of studies, a set of empirical rules, the Legon-Millen rules,[14-15] was formulated to rationalize the manner in which a protic acid binds to a Lewis base. Briefly, in a hydrogen bond formed between such species, the acid lies along the axis of a lone pair on its van der Waals partner. If no lone pairs are present, the acid lies along a perpendicular bisector of a π bond in the partner, as observed in ethylene–HX complexes (HX = HF,[16] HCl,[17] and HCCH[18]). A lone pair is preferred over a π pair; thus, in the case of vinyl fluoride complexes, the acid forms a hydrogen bond with the F atom in the substituted ethylene (HX = HF,[19] HCl,[20-21] and HCCH[22]). The hydrogen bond is not linear, but instead, bends from linearity to forge a secondary interaction with an electrophilic portion of the base,[23] which in these complexes, is the hydrogen atom located *cis* to the fluorine atom. A weaker hydrogen bond can bend more, giving, in general, a greater deviation from linearity.

These elegant results from the Legon group prompted us to ask further questions. What if we use the same acid but change the Lewis base? How is the nature of intermolecular interactions affected by changes in the electronic distribution of a subunit? How do different nucleophilic atoms in a subunit compete in affecting intermolecular interactions? What are the

effects of varying the electrophilicity of the hydrogen atoms? Fluoroethylenes with one or more hydrogen atoms provide distinctly different functionalities: both the π bond and the fluorine atoms are nucleophilic, but the hydrogen atoms are electrophilic. The hydrogen atoms in $C_2H_{4-n}F_n$ should be even more electropositive than those in C_2H_4 because of the electron withdrawing fluorine atoms. By increasing the number of fluorine substituents in ethylene, the double bond becomes less electron rich and the hydrogen atoms more electropositive, perhaps each to a different extent. We are, in effect, fine tuning the properties of the functional groups so that we can observe how they compete or cooperate with each other in intermolecular interactions. We can also easily alter the electronic distribution by including a chlorine atom, which is less electronegative and more polarizable than fluorine. The partners we choose for these haloethylenes are three protic acids: HF, HCl, and HCCH. Each can form a hydrogen bond, and each contains a nucleophilic region. Here, we report our systematic studies of these haloethylene-protic acid complexes, describe and discuss our findings, and the theoretical treatments we employ.

2. Experimental Methods

Protic acid-haloethylene heterodimers are formed in a pulsed jet expansion of a mixture of the two gases, typically 0.5 – 1.0% each diluted in argon, into vacuum (≈ 10^{-6} torr) through a nozzle with an 0.8 mm diameter orifice. Although some effort was made early on to optimize the mixture chemistry, this general recipe produces complexes in sufficient amounts for their structural characterization, and we now proceed without making any adjustments. Argon is used as the carrier gas, primarily due to its low cost compared to alternatives (helium or neon), but also we find stronger signals for the heterodimers in the argon expansion. The backing pressure of the pulsed-jet expansion is varied between 1 to 2 atm to produce optimal results. The many-

body collisions occurring in the high pressure region immediately downstream of the nozzle orifice serve both to form the heterodimers and, in argon, relax them to their lowest energy arrangement.[24-26] Typical rotational temperatures are 1 – 3 K. Low frequency vibrations (< ≈50 cm^{-1}) are likewise cooled, and higher frequency vibrations are expected to cool to approximately 50 – 100 K.[27-29]

Once formed, the rotational spectrum of the heterodimer is obtained using Fourier transform microwave (FTMW) spectroscopy. We use two such instruments in our work. The first is a broadband, chirped pulse FTMW spectrometer[30-32] based on the design introduced by Pate, *et al.*[33] In its current configuration, a 5 GHz arbitrary waveform generator (AWG) is used to create a 4 μs long pulse. The frequency of the AWG output is linearly swept from 4.5 (or 5.0) to 0.5 GHz over the duration of the pulse, which is mixed with one of three phase locked dielectric resonator oscillators (10.6 GHz, 14.6 GHz, 18.6 GHz). The lower sideband is isolated and amplified to 20 – 25 W of power to obtain the spectrum from 5.6 – 18.1 GHz in three portions (4.5 GHz for 5.6 – 10.1 GHz, 4.0 GHz for the other two bands), which are then stitched together, although variations on this theme have been used. The microwave pulse is timed to coincide with the arrival of the molecular sample from two pulsed valves between two microwave horn antennas. The sample is polarized by the pulse delivered through one antenna, and the resulting free induction decay (FID) is collected with the second antenna, and digitized at 50 Gs s^{-1} for 10 μs beginning 0.5 μs after the end of the polarization pulse. Ten FIDs are collected during each 800 μs opening of the pulsed valves, which typically operate at 4 Hz, although this is reduced to 0.8 Hz for overnight operation. 500,000 to 1,000,000 FIDs are averaged for each segment, and as described previously,[31] the average is Fourier transformed to give a frequency domain spectrum with a resolution element of 23.84 kHz and typical line

widths (FWHM) of 225 kHz. We have recently started digitizing the FID for 20 μs, which gives 11.92 kHz resolution elements and 110 kHz line widths. Frequency domain spectra from the broadband instrument are measured and analyzed using the AABS package of Kisiel,[34] available on the PROSPE website,[35-36] in conjunction with the SPFIT/SPCAT programs of Pickett.[37]

The second instrument is one of two narrowband, cavity-enhanced FTMW spectrometers of the Balle-Flygare design[38-40] in the laboratory,[31, 41] using the double heterodyne, quadrature phase modulation microwave circuit of Grabow[42] and controlled using the FTMW++ software system from the same author.[43] These instruments utilize one 0.8 mm pulsed nozzle and operate in the 5 – 20 GHz range. The time-domain signal is background-corrected and typically digitized at 10 Ms s^{-1} for 2048 data points and zero-filled to a 4096-point record length before Fourier transformation to give a frequency domain spectrum with a 2.4 kHz resolution element and linewidths on the order of 5 – 10 kHz. For weaker transitions or if hyperfine interactions are not present, it is often advantageous to digitize and zero-fill to half as many points, resulting in a doubling of the resolution element. Because the molecular beam axis is parallel to the resonator axis, the spectral lines are Doppler doubled, and the rest frequency of the transition is taken to be the arithmetic mean of the frequencies of two Doppler components, which are measured using FTMW++, and entered by hand for analysis by SPFIT/SPCAT.

The two different types of spectrometers have complementary strengths. The broadband instrument provides a spectrum over the entire 5.6 – 18.1 GHz spectral range in usually just under two or three days while running more or less unattended. The spectrum contains transitions due to all species formed in the pulsed jet expansion: the two monomers, complexes of each with the carrier gas or with residual water in the sample system, homodimers, the desired heterodimers, and to a lesser extent, higher order clusters. One can always return to the spectrum

at a later date if it is realized that something of interest might be there. However, given our current setup, the resolution and sensitivity of the instrument are not as great as that of the narrowband instrument. The lower resolution can be an advantage in reducing the complexity of the spectrum due to unwanted small hyperfine effects such as nuclear spin-spin or spin-rotation interactions, but it makes it harder to isolate other closely-spaced lines that would provide useful information. The sensitivity of the broadband instrument is sufficient for observing many naturally occurring singly-substituted (and sometimes doubly-substituted) isotopologues of monomeric species, but we seldom, for example, observe ^{13}C isotopologues of heterodimers in the instrument.

In contrast, the narrowband instrument has much greater resolution and sensitivity, but provides only 1 to 2 MHz (that is, 0.001 to 0.002 GHz) of the spectrum at a time. It requires constant attention, mostly spent tuning the cavity, while taking final measurements. Although automated scanning is possible when searching for lines, this is not particularly robust, and is anyway more cumbersome than using the broadband instrument. Consequently, one never acquires a spectrum over the entire 5 – 20 GHz range, but rather a discontinuous series of 1 to 2 MHz windows containing lines of interest for a specific molecular system. If later on there is curiosity about what else might have been formed in the pulsed jet expansion of a given gas mixture, it is necessary to start from scratch. However, the instrument provides greater measurement precision, due to the smaller resolution element and narrower linewidths, and can also resolve more closely spaced lines. With its greater sensitivity, singly-substituted ^{13}C isotopologues of heterodimers are routinely observed.

We find it advantageous to use the instruments in a manner that combines their relative strengths. A broadband spectrum is first obtained and the spectrum of the normal isotopologue

(also of singly-substituted ^{37}Cl, if chlorine is present) of the heterodimer of interest is assigned and analyzed.[44] The experimental spectroscopic constants obtained in this analysis are compared to those predicted by quantum chemistry calculations and used to adjust those predicted for the less abundant isotopologues. This is sufficient to narrow the search range, typically to only a few MHz, for these species so that they are easily found using the narrowband instrument. If desired, the transitions observed in the broadband spectrum can be remeasured with greater precision using the narrowband spectrometer. If later on, one suspects that additional species of interest might have been present in the pulsed jet expansion, one can return to the broadband spectrum. We should note that our early work on the protic acid-haloethylene heterodimers (before about 2012) was done using only the narrowband instrument.

The analysis using SPFIT/SPCAT provides spectroscopic constants for the observed species. The heterodimers are exclusively near-prolate asymmetric top molecules, and we analyze the spectra primarily with the Watson *A* reduced Hamiltonian in the I^r representation.[45] Although the *A* reduction diverges in the prolate symmetric top limit, it has been the traditional choice in the field primarily for a historical reason of being less computationally expensive, having fewer off-diagonal matrix elements in the symmetric top basis. Its use continues so to facilitate comparison with earlier work. Even for complexes with asymmetry parameter values of $\kappa = -0.98$ (in the prolate symmetric top limit, $\kappa = -1$), we find that use of the more appropriate *S* reduced Hamiltonian, which does not suffer the same divergence issues, leads to such small differences in spectroscopic constants that the same structures are determined for the species regardless of the reduction used.[46] In either case, it is typical to determine all three rotational constants, *A*, *B*, and *C*, and all five quartic centrifugal distortion constants, Δ_J, Δ_{JK}, Δ_K, δ_J, and δ_K (or D_J, D_{JK}, D_K, d_1, and d_2 in the *S* reduction). Occasionally higher order centrifugal distortion

corrections are required, and often for the less-abundant isotopologues, insufficient data is obtained to determine all five quartic or any of the higher-order constants. In this latter case, the relevant values are fixed to those determined for the most abundant isotopologue. For complexes containing chlorine atoms or other quadrupolar nuclei ($I > ½$), terms appropriate to the nuclear electric quadrupole coupling interaction are added to the Hamiltonian. Because the vast majority of the heterodimers have a planar average structure, the symmetric, traceless interaction tensor has only three independent, non-zero values, χ_{aa}, χ_{bb}–χ_{cc}, and χ_{ab}. The first two constants are always determinable while the latter one, having only off-diagonal matrix elements, requires the close approach of two interacting rotational states to have a measurable effect on transition frequencies. Nevertheless, we are often able to determine a value. The Laplace condition, $\chi_{aa}+\chi_{bb}+\chi_{cc} = 0$, is used in reporting values for all three diagonal elements of the quadrupole coupling tensor.

With the spectroscopic constants in hand, specifically rotational constants for all observed isotopologues, zero-point vibrationally averaged structures are found by fitting structural parameters to moments of inertia using either Schwendeman's STRFTQ program[47] or Kisiel's equivalent STRFIT.[35, 48] For planar molecules, only two of the three equilibrium moments of inertia are independent $\left(I_a + I_b = I_c\right)$, and for zero-point averaged values, the inertial defect, $I_c - I_a - I_b$, differs from zero only as a result of vibrational motion. Consequently, only two rotational constants from each isotopologue can be used in the fitting process. The choice is made empirically for each heterodimer to give the best fit. The geometries of the individual monomers are assumed to be unaffected by the weak intermolecular interactions, and these are held fixed at their zero-point average values. Only intermolecular structural parameters are allowed to vary. The choice of these is also critical. Often "obvious" or chemically relevant

parameters result in fits with unacceptably large correlations. There is an art to choosing alternatives that will break the correlations, and more useful distances and angles are subsequently found geometrically or by using Kisiel's EVAL program.[35] Even so, it is sometimes not possible to determine all desired intermolecular structural parameters from inertial data alone. In these cases, hyperfine interactions, either nuclear quadrupole or nuclear spin-spin, can be useful in determining angles via the second-rank tensor projection of a monomer value into the principal inertial axis system of the heterodimer.[49] Finally, a Kraitchman analysis[50] for isotopically substituted atoms is useful for verification of structural results. The calculations can be easily implemented from the original paper[50] or secondary references,[51] but Kisiel does maintain a program (KRA) for this purpose.[35]

3. Quantum Chemistry Calculations

Our experimental work is guided by and the analysis of our results are informed by quantum chemistry calculations. In making an assignment of the rotational spectrum of a molecule it is very helpful, if not necessary, to have a good estimate of the transition frequencies expected, which in turn depend on the geometry expected for the species. In early work, chemical intuition was often sufficient to provide an adequate estimate for the structures of the protic acid-haloethylene (at that time, specifically fluoroethylene) heterodimers. As the systems became more complex and the structural possibilities became more varied, we turned to increasingly better levels of theory to guide us.

For structure prediction, we use the GAUSSIAN quantum chemistry package, currently GAUSSIAN 16,[52] and have found that *ab initio* calculations at the MP2/6-311++G(2d,2p) level of theory provides rotational constants within a few percent of the experimental values ultimately obtained. It is important to realize that even this small percent discrepancy can lead to deviations

of hundreds of MHz for transition frequencies that have linewidths of 0.01 – 0.10 MHz. These calculations can also provide predictions of nuclear electric quadrupole coupling constants, and having predicted hyperfine splitting patterns can often be extremely helpful in recognizing the corresponding rotational transition in the experimental spectrum. Interestingly, it has been our experience that the limiting factor in the accuracy of the predicted quadrupole coupling constants is the predicted geometry of the heterodimer, as this affects the projection of the relatively accurately calculated tensor of the monomer onto the inertial axes of the heterodimer.

Accurate determination of the heterodimer binding energy and of the relative energy ordering of the minima located on the potential energy surface, calculated as discussed later, would require correcting for both the basis set superposition error (BSSE) and for the different zero-point energy (ZPE) associated with each geometry. For purposes of assigning rotational spectra, these are typically not necessary. As noted above, in the argon expansion we only observe the structure corresponding to the global minimum on the potential energy surface,[24] and indeed for simpler systems, the minima are well separated in energy so that the lowest energy structure is predicted correctly without the inclusion of BSSE or ZPE. Recently for the more complicated systems, we find several alternative structures located within a few tens of cm^{-1} of each other, and we have begun exploring the effects of correcting for both BSSE and ZPE. To put everything on a common ground for this paper, we have recalculated, using a common methodology, the energies for the local minima of all heterodimers discussed. Specifically, using the MP2/6-311++G(2d,2p) model chemistry, a full optimization, including a relaxation of the monomer geometries from their isolated molecule values, is done to give E_{eqil}. The relaxation of monomer geometry is necessary for a proper calculation of ZPE, which is done using the harmonic approximation and resulting in $E_{ZPE} = E_{equl} + ZPE$. A counterpoise

calculation[53] is then done at this geometry to correct for BSSE, giving E_{BSSE}, and the corrected energy of the heterodimer is taken to be $E_{\mathrm{dimer}} = E_{ZPE} - E_{\mathrm{eqil}} + E_{\mathrm{BSSE}}$. This is equivalent to assuming that the ZPE is not affected by the BSSE correction.

We typically start work on a complex by performing "relaxed scans" of intermolecular interaction potential energy surfaces. In these, the monomer geometries are fixed at their ground state average structures and the protic acid is swept around the haloethylene in angular steps of 5° or so while the intermolecular separation and the orientation of the protic acid are allowed to optimize. An example is shown in Fig. 1. The system chosen is vinyl fluoride–HF, and although this complex is from the foundational work of the Legon group,[19] it provides a nice illustration of the process.

In this example, a coordinate system is placed with origin at the center of mass of the vinyl fluoride molecule and with (*x*, *y*, *z*) axes corresponding to the (*b*, *c*, *a*) inertial axes of the monomer.[54] The fluorine atom of the hydrogen fluoride molecule is then located at spherical polar coordinates (R, θ, φ) relative to this system. The spherical polar angles are stepped, each in 10° increments over the ranges $5° \le \theta \le 175°$ and $0° \le \varphi \le 180°$, and at each (θ, φ) pair, R and the location of the hydrogen atom of the hydrogen fluoride molecule (with bond length fixed at the monomer value) are allowed to vary to optimize the energy. Three minima are found, labelled (a), (b), and (c) in the figure. The global minimum, (a), at (θ, φ) ≈ (110°, 180°) corresponds to the experimentally observed structure.[19] Because the atom is adjacent to a double bond, one of the lone pairs on fluorine participates in the conjugated π system via an unhybridized p orbital, and the remaining valence orbitals may be considered to adopt sp^2 hybridization. Thus, the structure is in accordance with the Legon-Millen rules with the acid lying along the conventional direction of a lone pair on the sp^2 hybridized fluorine atom and

bending slightly away from linearity to form a secondary interaction with a hydrogen on vinyl fluoride. Higher in energy, 104 cm^{-1} and 346 cm^{-1} (50 cm^{-1} and 270 cm^{-1} after BSSE and ZPE correction), respectively, are two local minima, (b) and (c). Interestingly, these also correspond to structures included in the Legon-Millen rules. Local minimum (b) has the HF approximately located along the direction of the other lone pair on fluorine, while minimum (c) puts the HF above the π bond if not precisely along a perpendicular bisector. With approximate locations determined for minima on the potential energy surface, optimized structures are then determined for each. These calculations provide the rotational constants and the dipole moment vector necessary to predict a rotational spectrum.

Once the spectra are obtained and analyzed and a structure determined for the heterodimer, it is useful to have guidance regarding the various contributions to the intermolecular interactions to understand why one arrangement is preferred over another. For this purpose, we utilize symmetry-adapted perturbation theory (SAPT)[55] as implemented in the Psi4 program package.[56] This method separates the intermolecular interaction energy into electrostatic, induction, dispersion, and exchange terms. The first three are attractive at a potential minimum while the fourth is repulsive. We focus on the relative values of contributions calculated using a common model chemistry when making comparisons among different heterodimers, leaving aside questions concerning the best means for obtaining accurate calculations of these values, and we choose the same MP2/6-311++G(2d,2p) model chemistry used for structure prediction.

We also make use of mapped electrostatic potential surfaces that can be generated using Gaussian 16.[52] These are electron density isosurfaces for a molecule, typically the haloethylene, onto which is mapped a color scale corresponding to the (signed) value of the electrostatic

potential at each point. These allow one to visualize and compare which regions of the molecule are electrostatically negative (and thus nucleophilic) or positive (electrophilic). In constructing these diagrams, we ensure that each uses a common value for the electron density defining the surface and a common color scale for the electrostatic potential.

4. Results

The experimental, average structures of the 22 haloethylene-protic acid complexes investigated in our group, together with those of the 3 vinyl fluoride complexes[19-21] and 1,1-difluoroethylene–HCl[57] studied by the Legon group, generally fall within one of three effectively planar motifs. Two of these motifs involve two interactions. A primary hydrogen bond is formed between the acid and a halogen atom in the haloethylene subunit, and this bond bends to allow a secondary interaction between the nucleophilic portion of the acid and a hydrogen atom[22] in the haloethylene. We call the motifs "top binding" and "side binding" when the secondary interaction involves the hydrogen atoms located respectively *cis* and geminal to the hydrogen bonded halogen atom. "Top" and "side" are useful, convenient terms meant to succinctly describe the binding modes despite the fact that they have no absolute reference aside from the way we have conventionally drawn the heterodimers, placing the C=C double bond horizontally. The top binding mode of vinyl fluoride–HF where HF binds across the double bond is illustrated in Fig. 1a. This is the structure observed experimentally by the Legon group. A higher energy isomer, discussed above, exhibits the side binding mode. Here HF would bind to hydrogen and fluorine atoms bonded to the same carbon atom, as shown in Fig. 1b.

The third binding motif does not share the common feature of primary and secondary interactions seen in top and side binding. In this third motif, only the hydrogen atom of the acid participates in the heterodimer formation, interacting with a pair of halogen atoms (not

necessarily equally) in a *cis* arrangement about the double bond of haloethylene, and the nucleophilic portion of the acid does not participate. This mode is observed in *cis*-1,2-difluoroethylene–HCl,[58] as shown in Fig. 2 and we call this "bifurcated".

Except for *trans*-1,2-difluoroethylene–HCCH, which has not yet been observed experimentally because its dipole moment is expected to be very small, the top binding mode has been observed exclusively for complexes of all three protic acids with three sets of fluoroethylene complexes: vinyl fluoride,[19-22] 1,1-difluoroethylene,[57, 59-60] and *trans*-1,2-difluoroethylene.[61-62] For 1,1,2-trifluoroethylene, however, only the side binding motif has been observed.[63-65] It is interesting to note that for these four sets of complexes, the binding motifs are independent of acid identity, but of course, the structural parameters are different, and they disclose the details concerning the strengths of the interactions, which will be discussed further in the next section. While 1,1-difluoroethylene offers only one motif (top), the other three fluoroethylenes could interact with an acid in the top or side binding motifs. It is informative to consider why a common, single motif is the lowest energy configuration for all three acids.

In a vinyl fluoride-acid complex, both top and side binding motifs would involve the same primary interaction: a hydrogen bond between the acid and the single fluorine atom. Thus, the determining factor for a stable configuration is provided by the secondary interaction. Specifically, the difference in electropositivity for the hydrogen atoms located *cis* and geminal to the fluorine atom as well as the feasibility for the nucleophilic portion of the acid of approaching them should be considered. Chemical intuition suggests that the geminal hydrogen, because of its proximity to the nucleophilic fluorine atom, should be more electropositive than the one located *cis* to (and three bonds away from) the fluorine atom. This is confirmed theoretically by mapping the electrostatic potential of vinyl fluoride onto its total electron density surface (Fig.

3a). Consequently, the side binding mode should be more favorable electrostatically than the top binding mode. The fact that side binding is not observed must have to do with the feasibility of attaining this mode and there are two factors to consider. First, does the electron density about the fluorine atom favor one mode over the other? Then, because the secondary interaction is achieved by bending the primary bond, which weakens it, it is important to consider the differences in the deviation of linearity of the hydrogen bond needed to adopt the two modes. We group these two feasibility factors under the broad category of steric effects. Ultimately, their origin is electronic, but our use of this term has the connotation of assessing the ease of a complex finding its way into a particular mode, or how well the two monomers "fit" together in this manner. In the case of the vinyl fluoride complexes, the observed values of the (top binding) CF···H angle are ~120°, which is in accord with the simple picture of an sp^2 hybridized fluorine atom, with one of the three lone pairs occupying an unhybridized p orbital perpendicular to the fluoroethylene plane so to overlap with the C=C bond. If we take the lengths of the primary and secondary interactions in each observed vinyl fluoride complex as yielding the most stable configuration, then using vinyl fluoride–HF as an example, obtaining these same lengths in the side binding configuration would require that the value of the CF···H angle be smaller and/or the hydrogen bond deviate more from linearity. Neither is stabilizing. Thus, we can conclude that the steric factors for the side binding mode are so unfavorable that the stronger electrostatic interactions in the ideal secondary interaction cannot compensate for it. As a result, only the top binding mode is observed.

In the case of 1,1,2-trifluoroethylene complexes, both the top and side binding modes involve the same hydrogen atom. The primary hydrogen bond is therefore the determining factor for the stability of each complex. The observed structures for all three complexes are side

binding, which, as described above, is more strained than a top binding configuration. In fact, the observed values of the CF···H angle are between 105° – 110°, and the angles of deviation from linearity of the hydrogen bond are between 42° and 69°. If these complexes were to have a top binding mode, then the values of the CF···H angle could remain 120° and the hydrogen bond deviate less from linearity. Since the steric factors in the observed structure are less favorable than for a putative top binding configuration, we can conclude that side binding for 1,1,2-trifluoroethylene must be driven by electrostatic factors. Indeed, mapping the electrostatic potential onto the total electron density surface of the molecule (Fig. 3b) shows that the fluorine atom geminal to the hydrogen atom is more nucleophilic than the one in the *cis* position.

The balance between steric and electrostatic factors can be directly examined using *trans*-1,2-difluoroethylene complexes. This fluoroethylene offers both top and side binding modes to an acid, but because of its symmetry, the two fluorine atoms are electrostatically equivalent, and the same is true for the two hydrogen atoms. Both binding modes, therefore, offer the same electrostatic factors. It follows then the observed configurations are the more sterically stable ones. Indeed, HF and HCl complexes of *trans*-1,2-difluoroethylene[61-62] both exhibit the top binding configuration, confirming our assessment that the side binding configuration for HF and HCl is sterically less favorable for a fluoroethylene than the top binding configuration. The complex with HCCH, as mentioned earlier, has not yet been studied, but we believe the same conclusion would be found for this acid.

The last remaining fluoroethylene, *cis*-1,2-difluoroethylene, does not present a top binding mode to an acid. It is, therefore, not surprising that HCCH binds to it in a side-binding motif.[66] The complex with HCl, however, adopts the third motif where H in the acid interacts with both F atoms.[58] In this bifurcated structure, the two hydrogen bonds are of significantly

different lengths [2.0730(3) Å and 2.9360(3) Å], and hence very different strengths. According to theory, this configuration is 80 cm^{-1} (BSSE and ZPE corrected) lower in energy than the side binding configuration, which leads us to speculate that the steric factors in the side binding configuration are much more restrictive for HCl than HCCH. This arises likely because the nucleophilic portion of the acid for HCl is located closer to the hydrogen atom involved in the primary interaction than is the one in HCCH (1.28 Å vs 1.66 Å). In forging a secondary interaction with the geminal hydrogen, HCl would have to bend so much from linearity to destabilize the hydrogen bond sufficiently to render the bifurcated motif the preferred arrangement. The weaker hydrogen bonding of the HCCH complex could also be a contributing factor in placing greater weight on the secondary interaction in determining the overall stability of the species.

Although the fluorine atom is more electronegative, the next heavier halogen, chlorine, is more polarizable. We seek to investigate how they differ from each other in modulating intermolecular interactions. The differences are particularly striking in the structures of vinyl chloride-acid complexes. When the acid is HF, the binding motif to vinyl chloride is top binding,[67] similar to the motif found for vinyl fluoride, except for one major difference: HF forms an angle of 102.4(2)° with the C–Cl bond, much smaller than the angle of 121.4° it forms with the C–F bond in vinyl fluoride. The small CCl···H angle indicates that the electronic distribution about chlorine is quite different from that about fluorine. This is confirmed by mapping the electrostatic potential surface onto the total electron density of vinyl chloride (Fig. 3c) and comparing it with that of vinyl fluoride. The most negative potential in vinyl chloride is located on a band centered about the chlorine atom, more or less perpendicular to the C–Cl bond. In contrast, the most negative potential in vinyl fluoride points away from the fluorine along the

C–F bond. The fact that HF adopts a top binding configuration to vinyl chloride suggests that this is sterically more favorable than the side binding configuration in which the fluorine atom of HF could interact with the more electropositive hydrogen geminal to the chlorine atom.

Unlike vinyl fluoride-acid complexes in which the binding mode is acid independent, the HCl and HCCH complexes of vinyl chloride do not adopt the same planar, top binding mode as their HF counterpart. HCl does bind to the *cis* Cl, H pair in vinyl chloride (thus top binding in a sense), but in a nonplanar fashion,[68-69] which is the first, and so far, the only example we have observed in haloethylene-acid complexes. This species exhibits a tunneling interconversion motion between the two equivalent geometries on alternate sides of the ethylene plane, greatly complicating the already congested hyperfine structure (due to the presence of two chlorine nuclei) for each rotational transition, and the spectroscopic work and analysis are on-going. HCCH adopts yet another configuration with vinyl chloride: a side-binding motif,[70] enabling the interaction between the nucleophilic C≡C bond and the more electropositive hydrogen geminal to chlorine. This motif is made possible by the relaxed steric requirements of chlorine, once again confirmed by the mapped electrostatic potential shown in Fig. 3c: the acid can approach the C–Cl bond at a smaller angle than it can for a C–F bond because of the different electron density distributions about chlorine and fluorine. In fact, the CCl···H angle is 88.67(22)°, much smaller than typical side-binding angle formed by an acid with a geminal F, H pair (104° – 110°), bringing the acetylenic bond closer to the hydrogen atom geminal to chlorine.

The haloethylenes we employ to examine the competition between fluorine and chlorine must, of course, contain these atoms and at least one hydrogen atom (to provide at least one possible site for a secondary interaction). We choose to use only those haloethylenes with one chlorine atom to avoid the spectral congestion due to additional nuclear quadrupole hyperfine

interactions. We have studied many, but not all, acid complexes with these monochlorofluoroethylenes, $C_2H_{3-n}F_nCl$, n = 1,2. Work is ongoing to complete systematically this series of heterodimers. Here, we generalize the results we have obtained so far. When the possibility for top binding to fluorine is present in a dihaloethylene (containing one fluorine and one chlorine), an acid invariably chooses to bind in this manner. Specifically, in all three 1-chloro-1-fluoroethylene–HX (HX = HF,[71] HCl,[72] HCCH[73]) complexes, the top binding mode to chlorine is not seen, and in (*E*)-1-chloro-2-fluoroethylene, binding to chlorine (both top and side) and side binding to fluorine are not observed for HF[74] and HCl.[49]

In the trihaloethylene, (*E*)-1-chloro-1,2-difluroethylene, where top binding to chlorine and side binding to fluorine are the available motifs, both HF[75] and HCCH[76] adopt the side binding mode similar to their 1,1,2-trifluoroethylene counterparts.[63, 65] This is because, as is the case in 1,1,2-trifluoroethylene, the fluorine atom geminal to the hydrogen atom in (*E*)-1-chloro-1,2-difluoroethylene is the most nucleophilic and the electrostatic advantage of the side binding mode appears to more than offset the unfavorable steric factors.

Several complexes do yield somewhat unexpected structures, at least at first glance. With side binding to chlorine and top binding to fluorine available, HCCH binds to chlorine in 2-chloro-1,1-difluoroethylene.[66] The chlorine and fluorine pair *trans* to each other are similarly nucleophilic (Fig. 3d); thus, the side binding to chlorine indicates that HCCH simply fits better in this configuration. When the top binding mode to fluorine is not present, such as in (*Z*)-1-chloro-2-fluoroethylene, HCCH again adopts a side binding configuration to chlorine and not choosing fluorine even though it is more nucleophilic.[77] Once again, HCCH appears to have a steric preference for side binding to chlorine rather than to fluorine. An entirely different mode is

adopted by HCl when binding to this haloethylene; it adopts the bifurcated motif, interacting with the fluorine and chlorine atoms.[78]

5. Discussion

In addition to the broad conclusions regarding the factors contributing to the overall structural motif adopted by each protic acid-haloethylene heterodimer discussed in the previous section, a subtler understanding of the nature of the intermolecular interactions can be reached with a more detailed comparison of structural parameters and trends. In general, a shorter hydrogen bond (typically F···H–X) is interpreted as a stronger interaction. The hydrogen bond prefers a linear arrangement, but deviates from linearity to gain additional stability, at the expense of the hydrogen bond, from an interaction between the nucleophilic part of the acid (F, Cl, or C≡C) and a hydrogen atom on the haloethylene.[23] We continue to call this latter interaction the secondary interaction, a term coined in some of the original work on these complexes, even when it appears that it might confer more stability to the species than does the hydrogen bond. The secondary interaction is likewise interpreted to be stronger when shorter, although comparisons between different acids must take into account the different van der Waals radii of each. The deviation of the hydrogen bond from linearity is also correlated with hydrogen bond strength. A weaker hydrogen bond will deviate more from linearity, both because less is lost in doing so and because it allows for a shorter, stronger secondary interaction. Tables 1 and 2 contain the binding motif, hydrogen bond length, CF(or Cl)···H angle, deviation from linearity, and secondary interaction length for protic acid-haloethylene heterodimers with fluorine and chlorine atom hydrogen bond acceptors, respectively.

Restricting our attention to heterodimers with a fluorine atom hydrogen bond acceptor, the top panel of Fig. 4 compares the hydrogen bond lengths for all observed species indexed by

increasing bond length for the HF complex. (Only the HCCH complex has been characterized for *cis*-1,2-difluoroethylene. It is placed by comparison with other HCCH complexes.) We note first that the hydrogen bond lengths reflect the gas phase acidity of the three acids. The HF complex always has the shortest bond length, the HCCH complex the longest, and the HCl complex lies between those two. Secondly, we observe that the HCl and HCCH complexes follow the same general trend in hydrogen bond length as do the HF complexes, indicating that the haloethylenes are arranged in order of decreasing strength as hydrogen bond acceptors. It is satisfying that this arrangement agrees with chemical intuition. Namely, the haloethylenes are grouped together in order of increasing halo-substitution. Going from left to right in the figure, there is vinyl fluoride (mono substituted), two (*E*)-substituted species, two 1,1-substituted species, the one *cis* or (*Z*) species, and finally two tri-substituted haloethylenes.

We conclude that increasing halo-substitution leads to a weakening of the hydrogen bond, and we attribute this to a decrease in nucleophilicity of the hydrogen bond acceptor atom due to electron withdrawal by the increasing number of electronegative atoms on the ethylene. Placing an additional halogen atom geminal to the acceptor has a greater effect than locating it in the *trans* position. The effect of an additional halogen *cis* to the acceptor cannot be definitively assessed because there is only one example, *cis*-1,2-difluoroethylene-HCCH. Clearly, determining the bonding motif and the hydrogen bond lengths in *cis*-1,2-difluoroethylene–HF and (*Z*)-1-chloro-2-fluoroethylene–HF are critical for verifying both the placement of this haloethylene between the 1,1- and tri-substituted species and the relative effects of *cis* versus *trans* versus geminal halogen substitution, but as discussed below, these complexes present challenges to their characterization. When comparing the effect of substituting chlorine versus fluorine, it appears that for a *trans* substitution relative to the hydrogen bond accepting fluorine

atom, there is little if any difference between the two halogens. The very small differences in the hydrogen bond lengths for the HF complexes of *trans*-1,2-difluoroethylene and (*E*)-1-chloro-2-fluoroethylene and those for the HCCH complexes of 1,1,2-trifluoroethylene and (*E*)-1-chloro-1,2-difluoroethylene suggest that *trans* chlorine substitution might have a marginally greater effect in decreasing the nucleophilicity of the hydrogen bond accepting fluorine atom than does fluorine substitution at that position. In contrast, there is a clear difference, seen with all three acids, in fluorine versus chlorine substitution geminal to the hydrogen bond accepting fluorine atom, and in this case it is fluorine that has the greater effect on hydrogen bond length. This is suggestive of differing importance for resonance versus inductive effects at the two positions.

The middle panel of Fig. 4 presents the secondary interaction bond lengths, with the haloethylenes arranged as before. The van der Waals radii of the chlorine atom (1.75 Å) and of the C≡C triple bond (1.78 Å) are similar to each other and both greater than that of the fluorine atom (1.47 Å).[79] Thus, it is to be expected that the secondary interaction length is always longer for HCl and HCCH than that for the corresponding HF species. However, the generally shorter lengths seen for HCCH complexes compared to their HCl analogues despite the slightly larger radius suggests that the secondary interaction is stronger in the HCCH complexes. Indeed, with the exception of vinyl fluoride, the difference between the secondary interaction length for HF and HCCH heterodimers with the same haloethylene is less than the difference in van der Waals radii (0.31 Å), implying that the secondary interaction is relatively more important in the case of HCCH complexes. The opposite is seen when comparing HF and HCl heterodimers. The differences in secondary interaction length for these species is greater than the difference in van der Waals radii (0.28 Å).

Comparing secondary interaction lengths for a common acid among the various haloethylenes, it is clear that an additional halogen placed geminal to the hydrogen atom involved in the secondary interaction, as in *trans*-1,2-difluoroethylene or (*E*)-1-chloro-2-fluoroethylene, has a dramatic effect on the secondary interaction strength. This can be attributed to an increased electropositivity of that hydrogen atom resulting from electron withdrawal by the halogen. It is somewhat puzzling, given the lesser electronegativity of chlorine, that the effect is so much greater in (*E*)-1-chloro-2-fluoroethylene than in *trans*-1,2-difluoroethylene, but this has been discussed in detail previously[49, 62] where the suggestion is made that resonance effects may be responsible. Nevertheless, with the exception of 1-chloro-1-fluoroethylene–HCl,[72] for which only a preliminary analysis has been done, the same trends in secondary interaction lengths are seen regardless of acid identity. Once again, this suggests that we are observing the effects of modulating the electron density of the haloethylene via halogen substitution.

The correlation between deviation from linearity and strength of the hydrogen bond is shown nicely in the bottom panel of Fig. 4. The deviation is always greatest for the most weakly bound HCCH complexes and the least for HF. With the exception of *trans*-1,2-difluoroethylene–HCl, the deviation from linearity generally tracks with the hydrogen bond length, and similarly substituted species have similar deviations from linearity. The observed deviation for *cis*-1,2-difluoroethylene–HCCH, which seems more in line with the tri-substituted haloethylene–HCCH species than those for the other di-substituted examples, can be understood by recalling that *cis*-1,2-difluoroethylene–HCCH has the side bound structural motif, in common with the tri-substituted halothylene complexes and not the top-binding motif seen for the other di-substituted examples.

There are only five examples of heterodimers with a chlorine atom hydrogen bond acceptor: each of the three acids (HF, HCl, HCCH) with vinyl chloride and the acetylene complexes of (*Z*)-1-chloro-2-fluoroethylene and of 2-chloro-1,1-difluoroethylene. Consequently, there is not as much to be gleaned from examining the observed structural trends. As noted earlier, unlike all the other species considered here, vinyl chloride–HCl has a non-planar average geometry. Thus, there are no similarly bound complexes for comparison, and it is not included in Table 2. Among the remaining four, the sole HF complex, vinyl chloride–HF, has the shortest hydrogen bond length, the smallest deviation from linearity, and the shortest secondary bond length. It is also the only planar top-binding species. The three side-binding complexes with acetylene also show the expected behavior. The hydrogen bond length increases with increasing halogen substitution as does the deviation from linearity, while the secondary bond length decreases with increasing halogen substitution, all while the CCl···H angle remains between 87 and 89 degrees.

Additional understanding of the factors contributing to the intermolecular interactions can be obtained with the help of theory, in particular, the energy decomposition provided by the SAPT calculations described earlier. In Fig. 5, we show the total SAPT interaction energy between the two subunits for each of the heterodimers we have observed. This includes those with a fluorine atom hydrogen bond acceptor discussed in the beginning of this section, arranged in the same monomer order. To these we add the species where chlorine is the hydrogen bond acceptor and also the two examples with a bifurcated hydrogen bond: HCl with both *cis*-1,2-difluoroethylene and (*Z*)-1-chloro-2-fluoroethylene. These additions are on the right side of the figure. Although the relative energies are more reliable than the absolute values, it is pleasing to see that all are in the range of typical hydrogen bonds, 8 – 23 kJ mol^{-1}. As inferred from the

structural parameters, HF complexes are more strongly bound than HCl complexes, which in turn are more strongly bound than HCCH ones. For complexes sharing a structural motif, there is a clear weakening of the intermolecular interactions with increasing halogen substitution. This is most readily seen for the first five subunits in the figure. The expected weakening in going from di-halo- to tri-halo-substituted species is offset by an increase in binding strength accompanying the switch from top binding to side binding. The two heterodimers with *cis*-1,2-difluoroethylene are interesting. The interaction strength for bifurcated *cis*-1,2-difluoroethylene–HCl is in line with those of other di-substituted haloethylenes despite not having a secondary interaction, and the binding energy for the side-bound *cis*-1,2-difluoroethylene–HCCH complex is similar to those of the side-binding 1,1,2-trifluoroethylene and (*E*)-1-chloro-1,2-difluoroethylene analogues. This latter effect, and the seemingly puzzling increase in interaction strength despite a weaker hydrogen bond for the HF complexes of trifluoroethylene and (*E*)-1-chloro-1,2-difluoroethylene are likely a result of an increased contribution from the secondary interaction to the binding energy. A similar explanation can be used for the increasing binding strength calculated for the series, vinyl chloride, (*Z*)-1-chloro-2-fluoroethylene, and 2-chloro-1,1-difluoroethylene with HCCH. Comparing with Table 2, the hydrogen bond length is increasing along the series, indicating a reduction in bond strength, but the secondary interaction length is rapidly decreasing, so much so to become shorter than the hydrogen bond.

The total SAPT interaction energy has four contributions,[55] electrostatic, induction, dispersion, and exchange. Of these, the first three are attractive; their sum is the total stabilization energy for the system. The exchange contribution is repulsive. We compare each of the various contributions to the interaction energy as an unsigned percentage of the total stabilization energy. For the heterodimers with a fluorine atom hydrogen bond acceptor, the

electrostatic interaction (top panel, Fig. 6) between permanent moments provides the majority of the stabilization energy, ranging from about 50 to 62%. The contribution decreases with increasing halogen substitution, in concert with the lengthening of the hydrogen bond. For side-binding (and bifurcated) species, the importance of the electrostatic contribution increases, by nearly 10%. Indeed, we have previously argued this based purely on structural interpretation and chemical intuition alone.[61, 63-65] For heterodimers with a chlorine atom hydrogen bond acceptor, the electrostatic contribution is less important, mostly less than 50% of the total stabilization energy, but an increase is seen for the series vinyl chloride, (*Z*)-1-chloro-2-fluoroethylene, and 2-chloro-1,1-difluoroethylene with HCCH, reflecting once again the increasing contribution from the secondary interaction, which comes to provide a significant portion of the binding energy. It is worth noting the two apparently strangely behaving HCl complexes, vinyl chloride–HCl and (*Z*)-1-chloro-2-fluoroethylene–HCl. The former, with the smallest contribution from electrostatics, is the only example of a non-planar heterodimer, while the latter is bifurcated. Thus, neither shares a binding motif with corresponding HF or HCCH complexes, and should not be expected to follow trends similar to the other examples.

The contributions from induction (middle panel, Fig. 6) are remarkable in their constancy, except in the case of vinyl chloride, which seems to be an exception to everything we have observed so far. In particular, each of the three protic acids adopts a different structural motif in binding to vinyl chloride. However, this monomer provides the only two cases where the two stronger and polar acids, HF and HCl, interact directly with the more polarizable chlorine atom. It could be that the 10% increase in the contribution from induction seen for vinyl chloride–HF and vinyl chloride–HCl compared to all other species is simply a reflection of the increased ease in distorting the electronic distribution around a polarizable chlorine atom. Not

being polar, HCCH would not cause a similar increase, while for bifurcated (*Z*)-1-chloro-2-fluoroethylene–HCl, the HCl interacts more strongly with fluorine than the chlorine atom. Nevertheless, induction is most important for HF complexes, contributing about 22% (29% for vinyl chloride) of the total stabilization energy. In HCl complexes, induction contributes 15 – 17% (23% for vinyl chloride) of the total stabilization energy, and drops to about 11% for HCCH complexes.

The contributions from dispersion appear to mirror those of electrostatics, and given the constancy of the induction contribution, this has to be the case, with the contribution from dispersion going up as that from electrostatics goes down. Not surprisingly, dispersion is least important for the HF-containing heterodimers and more important for HCl and HCCH species with a polarizable Cl atom or C≡C bond, respectively. With 25 to 40% of the total stabilization energy coming from dispersion, the importance of using post-Hartree Fock calculation methods for these species is readily apparent.

The three attractive interactions are opposed by the exchange repulsion (bottom panel, Fig 5) from the two approaching electron distributions associated with the two subunits. In general, this destabilization amounts to roughly 50 – 60% of the total stabilization effects, and once again there is remarkable constancy for a given acid across the series of haloethylenes, but with a few very informative exceptions. HF and HCCH show less exchange repulsion, while HCl generally has more. The notable exceptions are (yet again) vinyl chloride and the two bifurcated HCl species. The bifurcated species show the smallest (as a percentage of total stabilization energy) exchange repulsion. This suggests that this structural motif might be a consequence of providing smaller repulsive effects rather than stronger attractive forces. Sterically, HCl cannot achieve favorable electrostatics in the side binding motif, and in these two

haloethylenes, where top binding is not available, the secondary interaction is sacrificed for smaller exchange repulsion.

For the haloethylene-acid complexes that contain at least one fluorine and one hydrogen atom, and at most one chlorine atom, the structures of eleven species remain to be determined. Several of these heterodimers represent missing puzzle pieces that will address critical gaps in our understanding of the trends discussed above. We will continue to study these species, although many present particular challenges that must be overcome.

First and foremost, to possess an observable microwave spectrum, a species must have a dipole moment. Since neither *trans*-1,2-difluoroethylene nor HCCH is polar, they interact primarily via London dispersion forces with higher order multipole moments also making contributions. The binary complex will possess only a small, polarization-induced dipole moment regardless of the actual binding mode. Specifically, at the MP2/6-311++g(2d,2p) level of theory, the dipole moments of the top and side binding configurations for *trans*-1,2-difluoroethylene–HCCH are 0.07 D and 0.09 D, respectively. (The top binding configuration is predicted to be 42 cm^{-1} lower in energy.) With such a small dipole moment the species is not expected to be observable using the current configuration of the chirped pulse spectrometer. There is a possibility it can be observed using the more sensitive, narrowband Balle-Flygare spectrometer, but a lengthy and careful search process will be required.

A small dipole moment is also expected for (*E*)-1-chloro-2-fluoroethylene–HCCH. According to theory, the global minimum shows a side binding mode to chlorine, as observed experimentally for the complexes of HCCH with vinyl chloride,[70] (*Z*)-1-chloro-2-fluoroethylene,[77] and 2-chloro-1,1-difluroeothylene.[66] There is an isomer only 6 cm^{-1} higher in energy with HCCH top binding to fluorine, as observed for (*E*)-1-chloro-2-fluoroethylene–HF[74]

and (*E*)-1-chloro-2-fluoroethylene–HCl.[49] In both of these latter complexes, the secondary interaction is to the same hydrogen atom (geminal to chlorine and *cis* to fluorine). As a result, the identification of the experimental structure of (*E*)-1-chloro-2-fluoroethylene–HCCH would greatly help in teasing apart the competition between the more nucleophilic fluorine and the relaxed steric requirements of chlorine in binding to HCCH. The dipole moments of the side and top binding configurations for this complex are predicted to be 0.26 D and 0.22 D, respectively. Although these are larger than those predicted for the isomers of *trans*-1,2-difluoroethylene–HCCH, the quadrupolar chlorine atom will split each transition into, and distribute the intensity over, several hyperfine components. Once again, it is likely that we will only observe (*E*)-1-chloro-2-fluoroethylene–HCCH using the narrowband spectrometer.

Prior to constructing the chirped pulse spectrometer in one of our laboratories, we carried out an extensive search for the spectrum of *cis*-1,2-difluoroethylene–HF using the narrowband spectrometer. Despite this effort, we were not able to identify any transitions due to the most abundant isotopologue of this complex. However, using DF, we did observe normal *cis*-1,2-difluoroethylene–DF and two isotopologues singly substituted with ^{13}C, all of which are consistent with DF side binding to fluorine. The interaction potential energy surface for *cis*-1,2-difluoroethylene and HF has a shallow, extended valley connecting two minima corresponding to a side binding configuration and a bifurcated structure, respectively, and it is likely that the zero-point energy of the HF complex lies above the barrier connecting the two. Consequently, the structure is not localized, giving rise to a spectrum uncharacteristic of that for the global minimum (the side binding configuration). When DF is used in place of HF, however, the zero-point energy apparently is sufficiently lowered beneath the barrier, allowing us to observe the spectrum of the more stable binding mode. With the ability of the chirped pulse spectrometer to

cover a large spectral region simultaneously, we will return to the investigation of *cis*-1,2-difluoroethylene–HF with this instrument and attempt to identify its spectrum. Two other HF-containing complexes [(*Z*)-1-chloro-2-fluoroethylene–HF and 2-chloro-1,1-difluoroethylene–HF] also appear to have similar shallow, extended valleys, and their spectra therefore may also be more complicated than expected.

When the haloethylene contains a chlorine atom, the spectrum of its HCl-containing complex is complicated because each rotational transition is extensively split into many hyperfine components. We are in the process of finishing collecting and analyzing the spectra of two species: the HCl complexes of 1-chloro-1-fluoroethylene[72] and (*Z*)-1-chloro-2-fluoroethylene[78] and their preliminary structures are reported in a previous section. There remain three HCl-containing complexes to be investigated. Vinyl chloride–HCl, the only nonplanar complex, exhibits tunneling motions, making spectral assignment even more challenging.[68-69] In addition, we are encountering difficulties in analyzing the hyperfine components of some transitions, perhaps a result of some as yet unidentified perturbation. Quantum chemistry calculations predict that the HCl complexes with (*E*)-1-chloro-1,2-difluoroethylene and 2-chloro-1,1-difluoroethylene each have two isomers with similar energies (within 7 and 9 cm^{-1}, respectively, of each other). The lowest energy isomer for each is a side binding configuration, with HCl forming a hydrogen bond to fluorine with (*E*)-1-chloro-1,2-difluoroethylene and chlorine with 2-chloro-1,1-difluoroethylene. The higher energy structure, once again for each complex, is a bifurcated structure, with the H atom of HCl interacting with the F, F pair and the F, Cl pair, respectively, similar to the motifs observed for *cis*-1,2-difluoroethylene–HCl[58] and (*Z*)-1-chloro-2-fluoroethylene–HCl.[78]

(*Z*)-1-chloro-1,2-difluoroethylene has only recently become commercially available. Now that it is, we will able to study its heterodimers with HF, HCl, and HCCH. It is likely that these complexes will adopt a side binding structure, much like their 1,1,2-trifluoroethylene counterparts. In that case, comparisons among the trihaloethylene complexes will show the effect of replacing a fluorine atom in 1,1,2-trifluoroethylene with a chlorine atom. Specifically, comparing the heterodimers formed using (*Z*)-1-chloro-1,2-difluoroethylene to those with (*E*)-1-chloro-1,2-difluoroethylene will allow us to address the differences in placing the chlorine atom *trans* versus *cis* to the hydrogen bond acceptor.

6. Conclusions

The comparison of detailed structural parameters obtained via microwave rotational spectroscopy in a systematic study of protic acid-haloethylene heterodimers has provided a wealth of information regarding intermolecular interactions. This has been supplemented with information obtained from quantum chemistry calculations to refine our understanding of the contributions to complex formation. The observed structures, representative of the global minimum on the potential energy surface, reflect a balance between optimal electrostatics and steric requirements, *i.e.* how well the two interacting molecules fit together. In what we have termed "top-binding" to fluoroethylenes, the steric fit of HF, HCl, and HCCH, often allows overall stronger interactions than could be achieved to a more electropositive hydrogen atom available with side binding. Only in the tri-substituted haloethylenes can electrostatics contribute enough to the intermolecular interaction to overcome the "bad fit" of the side-binding configuration. The chlorine atom has relaxed steric requirements for hydrogen bonding, tipping the balance in the direction of electrostatics and allowing, in particular, several HCCH complexes to choose side-binding over an available top-binding option. However, the fit

remains bad enough for HCl, that in the two observed dihaloethylene–HCl complexes where top-binding is not an option, namely *cis*-1,2-difluoroethylene and (*Z*)-1-chloro-2-fluoroethylene, a bifurcated structure is adopted that appears to minimize the exchange repulsion.

The hydrogen bond acceptor strength of haloethylenes decreases in accord with chemical intuition as the degree of halogen substitution increased. This is accompanied by an increase in the electropositivity of the hydrogen atom participating in the secondary interaction. Both are a consequence of a greater degree of electron withdrawal by the additional halogens. This is verified by SAPT calculations that show both a decrease in binding energy and a lessening of the relative importance of electrostatics to the binding of heterodimers with a common structural motif upon increasing halogen substitution. In accord with conclusions reached using structural data and chemical intuition, electrostatics increases in importance upon switching to the side binding configuration.

All heterodimers with a hydrogen bond to fluorine show a similar relative contribution to binding from induction regardless of specific haloethylene identity that reflects the polarity of the acid, suggesting that the primary response is located at the halogen atom. The two species observed with a hydrogen bond involving a polar acid (HF or HCl) to chlorine show a significant enhancement of the contribution from induction, which is taken as supporting this conclusion. While the contribution from dispersion is significant for heterodimers containing HCl or HCCH, given the constancy of the induction contribution for the fluorine-bound species, this effect simply mirrors electrostatics. Likewise, the exchange repulsion is an approximately constant, common percentage of the total stabilization energy for a given acid in the top or side binding arrangements except for vinyl chloride, where the effect is a greater percentage for top binding, both planar (HF) and non-planar (HCl). Exchange repulsion is a very much smaller percentage

of total stabilization energy for bifurcated complexes of HCl, where the chlorine atom can remain relatively distant from the haloethylene.

There remain a few challenging heterodimers to observe and characterize, and doing so with provide essential information supporting or refuting some of the more speculative conclusions. These complexes remain active targets of investigation, and in particular, some of them have yet to be studied using the broadband, chirped pulse spectrometer. Others will take advantage of the recent easier availability of a few of the haloethylenes. Structure determination is an extremely effective means of obtaining information regarding chemical and molecular systems in general and on intermolecular interactions in particular.

7. Acknowledgements

This material is based on work supported by the National Science Foundation under Grants No. CHE-0234522, CHE-0517895, CHE-0809542, CHE-1111504, CHE-1465014, and CHE-1856637. HOL and MDM gratefully acknowledge the H. Axel Schupf ’57 Fund for Intellectual Life for support of the Faculty Research Awards Program at Amherst College and of sabbatical leaves. Over 50 undergraduate students have contributed to, and benefitted from, aspects of this work with support from the Amherst College Summer Science Undergraduate Research Fellowship Program and the Beckman Foundation, in addition to the previously mentioned funding sources.

8. Biographies

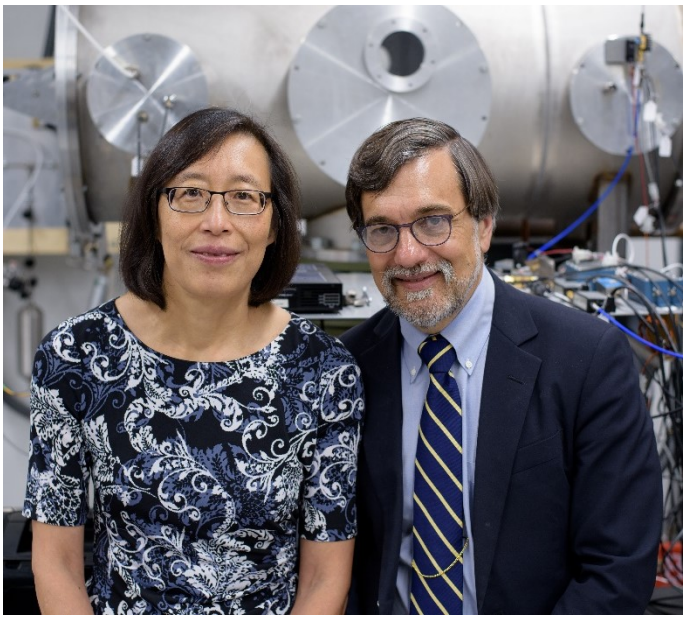

Helen O. Leung is the George H. Corey 1888 Professor of Chemistry at Amherst College. She received a B.S. in Chemistry (1982) and a B.A. in Biology (1983) from California State University Northridge. She continued to Harvard University receiving an M.A. (1985) and Ph.D. (1988) in the laboratory of William Klemperer. After a three-year postdoctoral fellowship at the Harvard-Smithsonian Center for Astrophysics, she spent two years as a Visiting Assistant Professor of Chemistry at Williams College before joining the faculty of Mount Holyoke College as an Assistant Professor in 1993 where she was promoted to Associate Professor in 1998. In 2002, she accepted a position at Amherst College as Professor of Chemistry and was named to her current position in 2009. Prof. Leung is the Chair-Elect of the International Advisory Committee for the International Symposium on Molecular Spectroscopy.

Mark D. Marshall is the Class of 1959 Professor of Chemistry at Amherst College. He received his B.S. in Chemistry from the University of Rochester in 1979 and an M.A. (1981) and Ph.D. (1985) from Harvard University in the research group of William Klemperer. After two years as a postdoctoral Research Associate at the Herzberg Institute of Astrophysics of the National Research Council Canada, he joined the faculty of Amherst College in 1987 as an Assistant Professor. He was promoted to Associate Professor in 1994 and Professor in 2000, and was

named to his current position in 2009. Prof. Marshall has served as a Councilor in the Chemistry Division of the Council on Undergraduate Research (CUR) and is currently Secretary to the CUR Executive Board.

Supporting Information Available: The complete citations for Gaussian 16 (Ref. 52) and PSI4 (Ref. 56) are available as supplementary material. This material is available free of charge via the Internet at http://pubs.acs.org.

References

1. Stone, A. J. *The Theory of Intermolecular Forces*. 2nd ed.; Oxford University Press: Oxford, 2013.

2. Clarke, A. G.; Smith, E. B. Low-Temperature Viscosities and Intermolecular Forces of Simple Gases. *J. Chem. Phys.* **1969,** *51*, 4156-4161.

3. Autumn, K.; Sitti, M.; Liang, Y. A.; Peattie, A. M.; Hansen, W. R.; Sponberg, S.; Kenny, T. W.; Fearing, R.; Isrealachvili, J. N.; Full, R. J. Evidence for Van Der Waals Adhesion in Gecko Setae. *Proc.Nat.Acad.Sci.* **2002,** *99*, 12252-12256.

4. Bermejo, I. A.; Usabiaga, I.; Compañón, I.; Castro-López, J.; Insausti, A.; Fernández, J. A.; Avenoza, A.; Busto, J. H.; Jiménez-Barbero, J.; Asensio, J. L., et al. Water Sculpts the Distinctive Shapes and Dynamics of the Tumor-Associated Carbohydrate Tn Antigens: Implications for Their Molecular Recognition. *J. Am. Chem. Soc.* **2018,** *140*, 9952-9960.

5. Copeland, R. A. *Enzymes: A Practical Introduction to Structure, Mechanism, and Data Analysis*. 2nd ed.; Wiley-VCH, Inc.: New York, 2000.

6. Berg, J. M.; Tymoczko, J. L.; Gatto, G. J., Jr.; Stryer, L. *Biochemistry*. 8th ed.; W.H. Freeman and Company: New York, 2015.

7. Ingold, C. K. Principles of an Electronic Theory of Organic Reactions. *Chem. Rev.* **1934,** *15*, 225-274.

8. Krygowski, T. M.; Stepien, B. T. Sigma- and Pi-Electron Delocalization: Focus on Substituent Effects. *Chem. Rev.* **2005,** *105*, 3482-3512.

9. Hankel, M.; Connor, J. N. L.; Schatz, G. C. Influence of Van Der Waals Wells on the Quantum Scattering Dynamics of the $Cl(^2P)+HCl \rightarrow ClH+Cl(^2P)$ Reaction. *Chem. Phys.* **2005,** *308*, 225-236.

10. Lakin, M. J.; Troya, D.; Schatz, G. C.; Harding, L. B. A Quasiclassical Trajectory Study of the Reaction $OH + CO \rightarrow H+CO_2$. *J. Chem. Phys.* **2003,** *119*, 5848-5859.

11. Skouteris, D.; Manolopoulos, D. E.; Bian, W. S.; Werner, H.-J.; Lai, L. H.; Liu, K. Van Der Waals Interactions in the Cl + HD Reaction. *Science* **1999,** *286*, 1713-1716.

12. Hansen, J. C.; Francisco, J. S. Radical-Molecule Complexes: Changing Our Perspective on the Molecular Mechanisms of Radical-Molecule Reactions and Their Impact on Atmospheric Chemistry. *Chemphyschem* **2002,** *3*, 833-840.

13. Westermann, T.; Kim, J. B.; Weichman, M. L.; Hock, C.; Yacovitch, T. I.; Palma, J.; Neumark, D. M.; Manthe, U. Resonances in the Entrance Channel of the Elementary Chemical Reaction of Fluorine and Methane. *Angew. Chem. Int. Ed.* **2014,** *53*, 1122-1126.

14. Legon, A. C.; Millen, D. J. Determination of Properties of Hydrogen-Bonded Dimers by Rotational Spectroscopy and a Classification of Dimer Geometries. *Faraday Discuss.* **1982,** *73*, 71-87.

15. Legon, A. C.; Millen, D. J. Angular Geometries and Other Properties of Hydrogen-Bonded Dimers: A Simple Electrostatic Interpretation of the Success of the Electron-Pair Model. *Chem.Soc.Rev.* **1987,** *16*, 467-498.

16. Shea, J. A.; Flygare, W. H. The Rotational Spectrum and Molecular Structure of the Ethylene-HF Complex. *J. Chem. Phys.* **1982,** *76*, 4857-4864.

17. Aldrich, P. D.; Legon, A. C.; Flygare, W. H. The Rotational Spectrum, Structure, and Molecular Properties of the Ethylene-HCl Dimer. *J. Chem. Phys.* **1981,** *75*, 2126-2134.

18. Fraser, G. T.; Lovas, F. J.; Suenram, R. D.; Gillies, J. Z.; Gillies, C. W. Microwave and Infrared Spectra of C_2H_4•••HCCH: Barrier to Twofold Internal Rotation of C_2H_4. *Chem. Phys.* **1992,** *163*, 91-101.

19. Cole, G. C.; Legon, A. C. A Characterisation of the Complex Vinyl Fluoride•••Hydrogen Fluoride by Rotational Spectroscopy and Ab Initio Calculations. *Chem. Phys. Lett.* **2004,** *400*, 419-424.

20. Kisiel, Z.; Fowler, P. W.; Legon, A. C. Rotational Spectrum, Structure, and Chlorine Nuclear Quadrupole Tensor of the Vinyl Fluoride-Hydrogen Chloride Dimer. *J. Chem. Phys.* **1990,** *93*, 3054-3062.

21. Legon, A. C.; Ottaviani, P. A Non-Linear Hydrogen Bond F•••H-Br in Vinyl Fluoride•••HBr Characterised by Rotational Spectroscopy. *Phys. Chem. Chem. Phys.* **2002,** *4*, 4103-4108.

22. Cole, G. C.; Legon, A. C. Non-Linearity of Weak B ••• H-C Hydrogen Bonds: An Investigation of a Complex of Vinyl Fluoride and Ethyne by Rotational Spectroscopy. *Chem. Phys. Lett.* **2003,** *369*, 31-40.

23. Legon, A. C. Non-Linear Hydrogen Bonds and Rotational Spectroscopy: Measurement and Rationalisation of the Deviation from Linearity. *Faraday Discuss.* **1994**, 19-33.

24. Klots, T. D.; Ruoff, R. S.; Gutowsky, H. S. Rotational Spectrum and Structure of the Linear CO_2-HCN Dimer: Dependence of Isomer Formation on Carrier Gas. *J. Chem. Phys.* **1989,** *90*, 4216-4216.

25. Emilsson, T.; Germann, T. C.; Gutowsky, H. S. Kinetics of Molecular Association and Relaxation in a Pulsed Supersonic Expansion. *J. Chem. Phys.* **1992,** *96*, 8830-8839.

26. Ruoff, R. S.; Klots, T. D.; Emilsson, T.; Gutowsky, H. S. Relaxation of Conformers and Isomers in Seeded Supersonic Jets of Inert Gases. *J. Chem. Phys.* **1990,** *93*, 3142-3142.

27. Smalley, R. E.; Wharton, L.; Levy, D. H. Molecular Optical Spectroscopy with Supersonic Beams and Jets. *Acc. Chem. Res.* **1977,** *10*, 139-145.

28. Schäfer, M.; Bauder, A. Vibrationally Excited States in a Pulsed Jet Observed by Fourier Transform Microwave Spectroscopy. *Chem. Phys. Lett.* **1999,** *308*, 355-362.

29. Maris, A.; Favero, L. B.; Danieli, R.; Favero, P. G.; Caminati, W. Vibrational Relaxation in Pyridine Upon Supersonic Expansion. *J. Chem. Phys.* **2000,** *113*, 8567-8573.

30. Marshall, M. D.; Leung, H. O.; Scheetz, B. Q.; Thaler, J. E.; Muenter, J. S. A Chirped Pulse Fourier Transform Microwave Study of the Refrigerant Alternative 2,3,3,3-Tetrafluoropropene. *J. Mol. Spectrosc.* **2011,** *266*, 37-42.

31. Marshall, M. D.; Leung, H. O.; Calvert, C. E. Molecular Structure of the Argon-(*Z*)-1-Chloro-2-Fluoroethylene Complex from Chirped-Pulse and Narrow-Band Fourier Transform Microwave Spectroscopy. *J. Mol. Spectrosc.* **2012,** *280*, 97-103.

32. Leung, H. O.; Marshall, M. D.; Messinger, J. P.; Knowlton, G. S.; Sundheim, K. M.; Cheung-Lau, J. C. The Microwave Spectra and Molecular Structures of 2-Chloro-1,1-Difluoroethylene and Its Complex with the Argon Atom. *J. Mol. Spectrosc.* **2014,** *305*, 25-33.

33. Brown, G. G.; Dian, B. C.; Douglass, K. O.; Geyer, S. M.; Shipman, S. T.; Pate, B. H. A Broadband Fourier Transform Microwave Spectrometer Based on Chirped Pulse Excitation. *Rev. Sci. Instr.* **2008,** *79*, 053103.

34. Kisiel, Z.; Pszczółkowski, L.; Medvedev, I. R.; Winnewisser, M.; deLucia, F. C.; Herbst, E. Rotational Spectrum of *Trans–Trans* Diethyl Ether in the Ground and Three Excited Vibrational States. *J. Mol. Spectrosc.* **2005,** *233*, 231-243.

35. Kisiel, Z. Prospe - Programs for Rotational Spectroscopy. http://info.ifpan.edu.pl/~kisiel/prospe.htm (accessed July 17, 2019).

36. Kisiel, Z., Assignment and Analysis of Complex Rotational Spectra. In *Spectroscopy from Space*, Demaison, J.; Sarka, K.; Cohen, E. A., Eds. Kluwer Academic Publishers: Dordrecht, 2001.

37. Pickett, H. M. The Fitting and Prediction of Vibration-Rotation Spectra with Spin Interactions. *J. Mol. Spectrosc.* **1991,** *148*, 371-377.

38. Balle, T. J.; Campbell, E. J.; Keenan, M. R.; Flygare, W. H. A New Method for Observing the Rotational Spectra of Weak Molecular Complexes: KrHCl. *J. Chem. Phys.* **1979,** *71*, 2723-2724.

39. Balle, T. J.; Campbell, E. J.; Keenan, M. R.; Flygare, W. H. A New Method for Observing the Rotational Spectra of Weak Molecular Complexes: KrHCl. *J. Chem. Phys.* **1980,** *72*, 922-932.

40. Balle, T. J.; Flygare, W. H. Fabry-Perot Cavity Pulsed Fourier Transform Microwave Spectrometer with a Pulsed Nozzle Source. *Rev. Sci. Instr.* **1981,** *52*, 33-45.

41. Leung, H. O.; Gangwani, D.; Grabow, J. U. Nuclear Quadrupole Hyperfine Structure in the Microwave Spectrum of Ar-N_2O. *J. Mol. Spectrosc.* **1997,** *184*, 106-112.

42. Grabow, J. U.; Stahl, W.; Dreizler, H. A Multioctave Coaxially Oriented Beam-Resonator Arrangement Fourier-Transform Microwave Spectrometer. *Rev. Sci. Instr.* **1996,** *67*, 4072-4084.

43. Grabow, J. U. Habilitationsschrift. Universität Hannover, Hannover, 2004.

44. These spectra are also very useful in providing “starter” projects to engage undergraduate students, who learn by assigning spectra of monomers and their complexes with the carrier gas.

45. Watson, J. K. G., Aspects of Quartic and Sextic Centrifugal Effects on Rotational Energy Levels. In *Vibrational Spectra and Structure*, Durig, J. R., Ed. Elsevier Scientific Publishing: Amsterdam, 1977; Vol. 6, pp 1-89.

46. If differences are observed, then the S reduction values are to be preferred.

47. Schwendeman, R. H., In *Critical Evaluation of Chemical and Physical Structural Information*, Lide, D. R.; Paul, M. A., Eds. National Academy of Science: Washington, DC, 1974.

48. Kisiel, Z. Least-Squares Mass-Dependence Molecular Structures for Selected Weakly Bound Intermolecular Clusters. *J. Mol. Spectrosc.* **2003,** *218*, 58-67.

49. Leung, H. O.; Marshall, M. D. Effect of Chlorine Substitution in Modulating the Relative Importance of Two Intermolecular Interactions: The Microwave Spectrum and Molecular Structure of (*E*)-1-Chloro-2-Fluoroethylene−HCl. *J. Phys. Chem. A* **2016,** *120*, 7955-7963.

50. Kraitchman, J. Determination of Molecular Structure from Microwave Spectroscopic Data. *Am. J. Phys.* **1953,** *21*, 17-24.

51. Gordy, W.; Smith, W. V.; Trambarulo, R. F. *Microwave Spectroscopy*. John Wiley & Sons: New York, 1953.

52. Frisch, M. J.; Trucks, G. W.; Schlegel, H. B.; Scuseria, G. E.; Robb, M. A.; Cheeseman, J. R.; Scalmani, G.; Barone, V.; Petersson, G. A.; Nakatsuji, H., et al. *Gaussian 16*, Revision A.03; Wallingford, CT, 2016.

53. Boys, S. F.; Bernardi, F. The Calculation of Small Molecular Interactions by the Differences of Separate Total Energies. Some Procedures with Reduced Errors. *Mol. Phys.* **1970,** *19*, 553-566.

54. This is not the only possibility. For example, we often put the origin at the center of the C=C bond, which is also taken to define the z-axis, with the haloethylene lying in the xz plane.

55. Jeziorski, B.; Moszynski, R.; Szalewicz, K. Perturbation Theory Approach to Intermolecular Potential Energy Surfaces of Van Der Waals Complexes. *Chem. Rev.* **1994,** *94*, 1887-1930.

56. Parrish, R. M.; Burns, L. A.; Smith, D. G. A.; Simmonett, A. C.; De Prince, A. E., III; Hohenstein, E. G.; Bozkaya, U.; Sokolov, A. Y.; Di Remigio, R.; Richard, R. M., et al. Psi4 1.1: An Open-Source Electronic Structure Program Emphasizing Automation, Advanced Libraries, and Interoperability. *J. Chem. Theory Comput.* **2017,** *13*, 3185-3197.

57. Kisiel, Z.; Fowler, P. W.; Legon, A. C. Investigation of the Rotational Spectrum of the Hydrogen-Bonded Dimer CF_2CH_2•••HCl. *J. Chem. Soc. Faraday Trans.* **1992,** *88*, 3385-3391.

58. Leung, H. O.; Marshall, M. D.; Yoon, L. H. The Importance of a Good Fit: The Microwave Spectra and Molecular Structures of *Trans*-1,2-Difluoroethylene-Hydrogen Chloride and *Cis*-1,2-Difluoroethylene-Hydrogen Chloride. The 72nd International Symposium on Molecular Spectroscopy, Talk TC-06, Urbana-Champaign, IL, 2017.

59. Leung, H. O.; Marshall, M. D.; Drake, T. L.; Pudlik, T.; Savji, N.; McCune, D. W. Fourier Transform Microwave Spectroscopy and Molecular Structure of the 1,1-Difluoroethylene–Hydrogen Fluoride Complex. *J. Chem. Phys.* **2009,** *131*, 204301.

60. Leung, H. O.; Marshall, M. D. Rotational Spectroscopy and Molecular Structure of the 1,1-Difluoroethylene-Acetylene Complex. *J. Chem. Phys.* **2006,** *125*, 154301.

61. Leung, H. O.; Marshall, M. D.; Amberger, B. K. Fourier Transform Microwave Spectroscopy and Molecular Structure of the *Trans*-1,2-Difluoroethylene–Hydrogen Fluoride Complex. *J. Chem. Phys.* **2009,** *131*, 204302.

62. Leung, H. O.; Marshall, M. D. Finding the Better Fit: The Microwave Spectrum and Sterically Preferred Structure of *Trans*-1,2-Difluoroethylene-Hydrogen Chloride. *J. Phys. Chem. A* **2018,** *122*, 8363-8369.

63. Leung, H. O.; Marshall, M. D. Rotational Spectroscopy and Molecular Structure of 1,1,2-Trifluoroethylene and the 1,1,2-Trifluoroethylene-Hydrogen Fluoride Complex. *J. Chem. Phys.* **2007,** *126*, 114310.

64. Leung, H. O.; Marshall, M. D.; Ray, M. R.; Kang, J. T. Rotational Spectroscopy and Molecular Structure of the 1,1,2-Trifluoroethylene-Hydrogen Chloride Complex. *J. Phys. Chem. A* **2010,** *114*, 10975-10980.

65. Leung, H. O.; Marshall, M. D.; Cashion, W. T.; Chen, V. L. Rotational Spectroscopy and Molecular Structure of the 1,1,2-Trifluoroethylene-Acetylene Complex. *J. Chem. Phys.* **2008,** *128*, 064315.

66. Leung, H. O.; Marshall, M. D. Tipping the Balance between Electrostatics and Steric Effects: The Microwave Spectra and Molecular Structures of 2-Chloro-1,1-Difluoroethylene–Acetylene and *Cis*-1,2-Difluoroethylene–Acetylene. The 73rd International Symposium on Molecular Spectroscopy, Talk TJ-06, Urbana-Champaign, IL, 2018.

67. Leung, H. O.; Marshall, M. D. The Effect of Acid Identity on the Geometry of Intermolecular Complexes: The Microwave Spectrum and Molecular Structure of Vinyl Chloride-HF. *J. Phys. Chem. A* **2014,** *118*, 9783-9790.

68. Messinger, J. P.; Leung, H. O.; Marshall, M. D. The Effect of Protic Acid Identity on the Structures of Complexes with Vinyl Chloride: Fourier Transform Microwave Spectroscopy and Molecular Structure of the Vinyl Chloride-Hydrogen Chloride Complex. The 69th International Symposium on Molecular Spectroscopy, Talk TE07, Urbana-Champaign, IL, 2014.

69. Leung, H. O.; Marshall, M. D.; Messinger, J. P. Chlorine Nuclear Quadrupole Hyperfine Structure in the Vinyl Chloride-Hydrogen Chloride Complex. The 70th International Symposium on Molecular Spectroscopy, Talk WJ06, Urbana-Champaign, IL, 2015.

70. Leung, H. O.; Marshall, M. D.; Feng, F. The Microwave Spectrum and Molecular Structure of Vinyl Chloride-Acetylene, a Side-Binding Complex. *J. Phys. Chem. A* **2013,** *117*, 13419-13428.

71. Leung, H. O.; Marshall, M. D.; Bozzi, A. T.; Cohen, P. M.; Lam, M. Microwave Spectrum and Molecular Structure of the 1-Chloro-1-Fluoroethylene-Hydrogen Fluoride Complex. *J. Mol. Spectrosc.* **2011,** *267*, 43-49.

72. Hoque, L.; Leung, H. O.; Marshall, M. D. The Microwave Spectrum and Molecular Structure of 1-Chloro-1-Fluoroethylene-Hydrogen Chloride. The 74th International Symposium on Molecular Spectroscopy, Talk TB-07, Urbana-Champaign, IL, 2019.

73. Leung, H. O.; Marshall, M. D.; Grimes, D. D. Rotational Spectroscopy and Molecular Structure of the 1-Chloro-1-Fluoroethylene-Acetylene Complex. *J. Chem. Phys.* **2011,** *134*, 034303.

74. Leung, H. O.; Marshall, M. D.; Lee, A. J. The Microwave Spectrum and Molecular Structure of (*E*)-1-Chloro-2-Fluoroethylene–HF: Revealing the Balance among Electrostatics, Sterics, and Resonance in Intermolecular Interactions. *J. Phys. Chem. A* **2016,** *120*, 7935-7946.

75. Bozzi, A. T.; Leung, H. O.; Marshall, M. D. Determining the Ground State Geometry of the (*E*)-1-Chloro-1,2-Difluoroethylene–Hydrogen Fluoride Complex Using Microwave Spectroscopy. The 65th International Symposium on Molecular Spectroscopy, Talk TH-13, Columbus, OH, 2010.

76. Leung, H. O.; Marshall, M. D. The Microwave Spectrum and Molecular Structure of (*E*)-1-Chloro-1,2-Difluoroethylene-Acetylene. The 74th International Symposium on Molecular Spectroscopy, Talk TB-02, Urbana-Champaign, IL, 2019.

77. Leung, H. O.; Marshall, M. D.; Khan, N. D. The Microwave Spectrum and Molecular Structure of (*Z*)-1-Chloro-2-Fluoroethylene–Acetylene: Demonstrating the Importance of the Balance between Steric and Electrostatic Interactions in Heterodimer Formation. *J. Phys. Chem. A* **2017,** *121*, 5651-5658.

78. Tandon, H. K.; Leung, H. O.; Marshall, M. D. Does a Second Halogen Atom Affect the Nature of Intermolecular Interactions in Protic Acid-Haloethylene Complexes? In (*Z*)-1-Chloro-2-Fluoroethylene It Most Certainly Does! The 71st International Symposium on Molecular Spectroscopy, Talk WG09, Urbana-Champaign, IL, 2016.

79. Bondi, A. Van Der Waals Volumes and Radii. *J. Phys. Chem.* **1964,** *68*, 441-451.

Table 1: Binding motif, hydrogen bond length, CF···H angle, deviation from linearity, and secondary interaction length for protic acid-haloethylene heterodimers with a fluorine atom hydrogen bond acceptor.

	Binding Motif	H···F / Å	CF···H / °	Deviation from Linearity / °	Secondary Interaction Length[a]/ Å	Ref.
CH_2CHF–HF	Top	1.892(14)	121.4	18.7(15)	2.734	19
CH_2CHF–HCl	Top	2.123(1)	123.7(1)	18.3(1)	3.162	20[b]
CH_2CHF–HCCH	Top	2.441(4)	122.6(4)	36.5(2)	3.159	22
trans-CHFCHF–HF	Top	1.910297(68)	118.4327(23)	21.65	2.6095(1)	61
trans-CHFCHF–HCl	Top	2.20030(53)	125.106(19)	30.72	3.0626(9)	62
(*E*)-CHClCHF–HF	Top	1.9399(19)	118.200(55)	24.75	2.4510(26)	74
(*E*)-CHClCHF–HCl	Top	2.19481(34)	122.2397(95)	27.37	2.9011(5)	49
CH_2CClF–HF	Top	1.9482(10)	124.371(70)	29.14	2.7386(19)	71
CH_2CClF–HCl	Top	2.1864(3)	130.539(71)	32.799(38)	3.2267(20)	72
CH_2CClF–HCCH	Top	2.623(11)	124.30(70)	52.82(28)	2.977(17)	73
CH_2CF_2–HF	Top	1.98833(44)	122.41	29.99	2.7825(3)	59
CH_2CF_2–HCl	Top	2.33094(36)	122.41	34.22	3.07619(30)	57[c]
CH_2CF_2–HCCH	Top	2.646(11)	122.41(79)	53.25(24)	3.005(21)	60
cis-CHFCHF–HCCH	Side	2.6455(92)	106.24(14)	63.85(34)	2.9654(25)	66
$CHFCF_2$–HF	Side	2.020(41)	109.0(13)	41.6(51)	2.7522(40)	63
$CHFCF_2$–HCl	Side	2.3416(7)	109.720(39)	47.729(13)	3.0796(5)	64
$CHFCF_2$–HCCH	Side	2.748(15)	104.49(15)	69.24(67)	2.8694(9)	65
(*E*)-CClFCHF–HF	Side	2.02(2)	109.2(6)	42(2)	2.757(1)	75
(*E*)-CClFCHF–HCCH	Side	2.7704(98)	104.763(74)	70.59(43)	2.8601(2)	76

[a]The secondary interaction length refers to the distance between the nucleophilic portion of the acid, namely, F, Cl, or the center of the acetylenic bond for HF, HCl, and HCCH, respectively, and the nearest hydrogen atom in the fluoroethylene subunit.

[b]Structure refitted in Ref. 21

[c]Structure refitted in Ref. 59

Table 2: Binding motif, hydrogen bond length, CCl···H angle, deviation from linearity, and secondary interaction length for protic acid-haloethylene heterodimers with a chlorine atom hydrogen bond acceptor or adopting a bifurcated motif.

	Binding Motif	H···Cl / Å	CCl···H / °	Deviation from Linearity / °	Secondary interaction length[a]/ Å	Ref.
CH_2CHCl–HF	Top	2.319(6)	102.4(2)	19.8	2.59(1)	67
CH_2CHCl–HCCH	Side	3.014(14)	88.67(22)	58.49(54)	2.9392(41)	70
(*Z*)-CHClCHF–HCl	Bifurcated	2.191(2)[b] 3.096(2)[c]	135.27(5)[d]	7.06(5)		78
(*Z*)-CHClCHF–HCCH	Side	3.0690(89)	87.843(97)	62.44(43)	2.7815(8)	77
CF_2CHCl–HCCH	Side	3.185(11)	87.204(79)	68.66(49)	2.7214(2)	66
cis-CHFCHF–HCl	Bifurcated	2.0730(3)[e] 2.9360(3)[e]	131.65(1)[d]	1.791(4)		58

[a]The secondary interaction length refers to the distance between the nucleophilic portion of the acid, namely, F, Cl, or the center of the acetylenic bond for HF, HCl, and HCCH, respectively, and the nearest hydrogen atom in the haloethylene subunit. The bifurcated complexes do not have a secondary interaction.

[b]This is the H···F distance in the bifurcated hydrogen bond.

[c]This is the H···Cl distance in the bifurcated hydrogen bond.

[d]This is the CF···H angle of the shorter hydrogen bond.

[e]In the zero-point averaged structure, the two hydrogen bonds in *cis*-CHFCHF–HCl are of unequal lengths, although the ground state wave function is the symmetric combination of two equivalent configurations.

Figure 1. A relaxed scan of the intermolecular potential energy surface for the vinyl fluoride–HF heterodimer. The position of the fluorine atom of HF is located relative to the principal inertial axis system of vinyl fluoride by the spherical polar coordinates (R, θ, φ). When θ and φ are both equal to zero, the fluorine atom lies on the positive z axis (coincident with the a axis of the inertial axis system for vinyl fluoride) at a distance R from the center of mass. The two angles are scanned in steps of 10° while the distance, R, and the location of the hydrogen atom of HF (with fixed HF bond length) are allowed to vary to minimize the energy. Structures (a), (b), and (c) correspond to the similarly labelled minima on the surface. Structures (a) and (b) are examples of what we term "top-binding" and "side-binding," respectively. They are labelled with the geometric parameters discussed in the text: hydrogen bond length ($r_{primary}$), secondary bond length ($r_{secondary}$), deviation from linearity (δ), and CX···H angle (α), X = F or Cl.

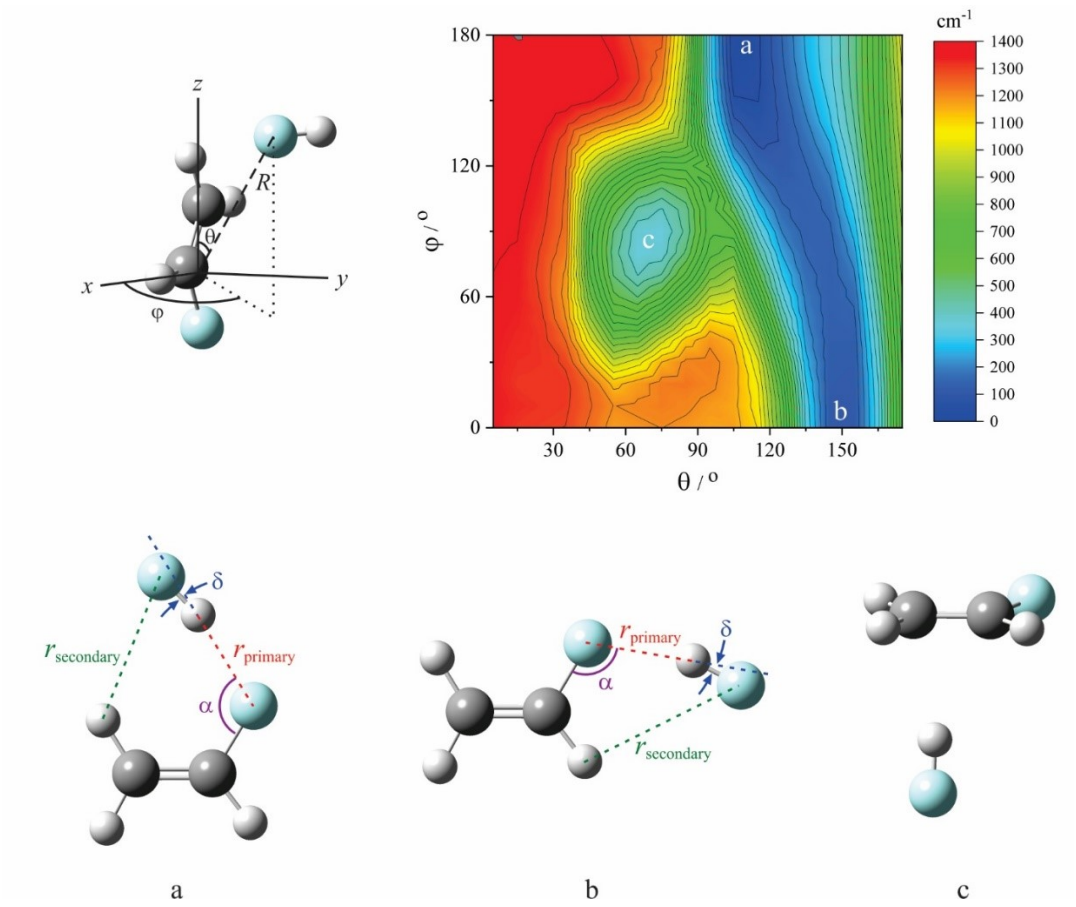

Figure 2. Structures for all observed protic acid-haloethylene gas phase heterodimers discussed in this paper. Bond lengths and angles are drawn to scale.[a] Gray boxes indicate heterodimers yet to be characterized.

	HF	HCl	HCCH		HF	HCl	HCCH
CH_2CHF	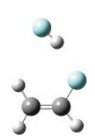	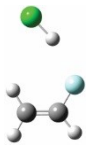	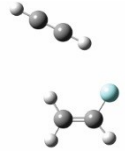	$CHFCF_2$	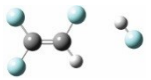		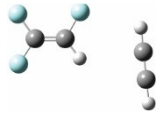
trans-CHFCHF	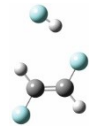	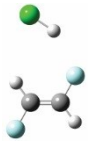		(*E*)-CClFCHF	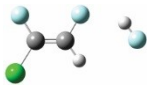		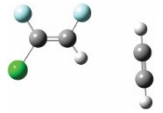
(*E*)-CHClCHF	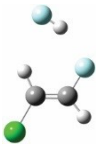	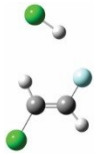		CH_2CHCl	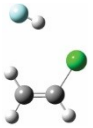	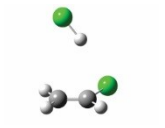	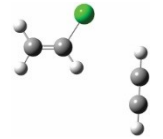
CH_2CClF	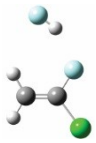	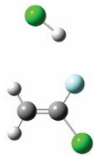	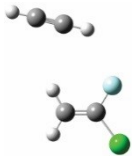	(*Z*)-CHClCHF	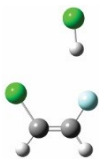	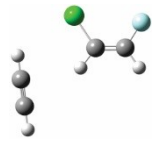	
CH_2CF_2	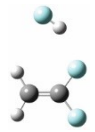	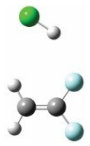	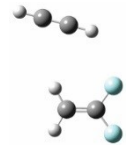	CF_2CHCl		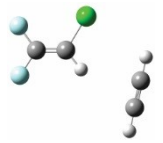	
cis-CHFCHF		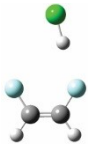	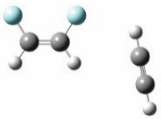				

[a]The precise values for the geometric parameters for the HCl complexes of CH_2CClF, *cis*-CHFCHF, CH_2CHCl, (*Z*)-CHClCHF, and all observed heterodimers of (*E*)-CClFCHF and (*Z*)-CClFCHF are subject to refinement as final analysis of the data is completed.

Figure 3. Mapped electrostatic potential surfaces, as described in the text, for (a) vinyl fluoride, (b) 1,1,2-trifluoroethylene, (c) vinyl chloride, and (d) 2-chloro-1,1-difluoroethylene. A common value of the electron density and common color scale, in which red is the most negative and blue the most positive, is used for each diagram.

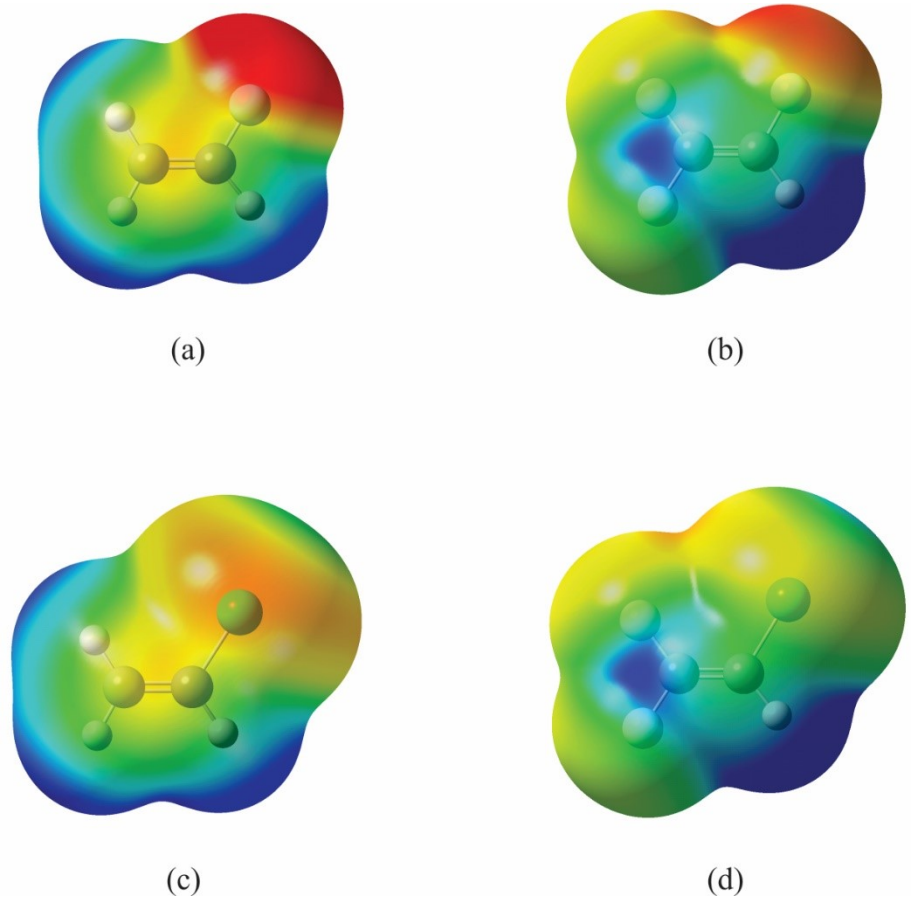

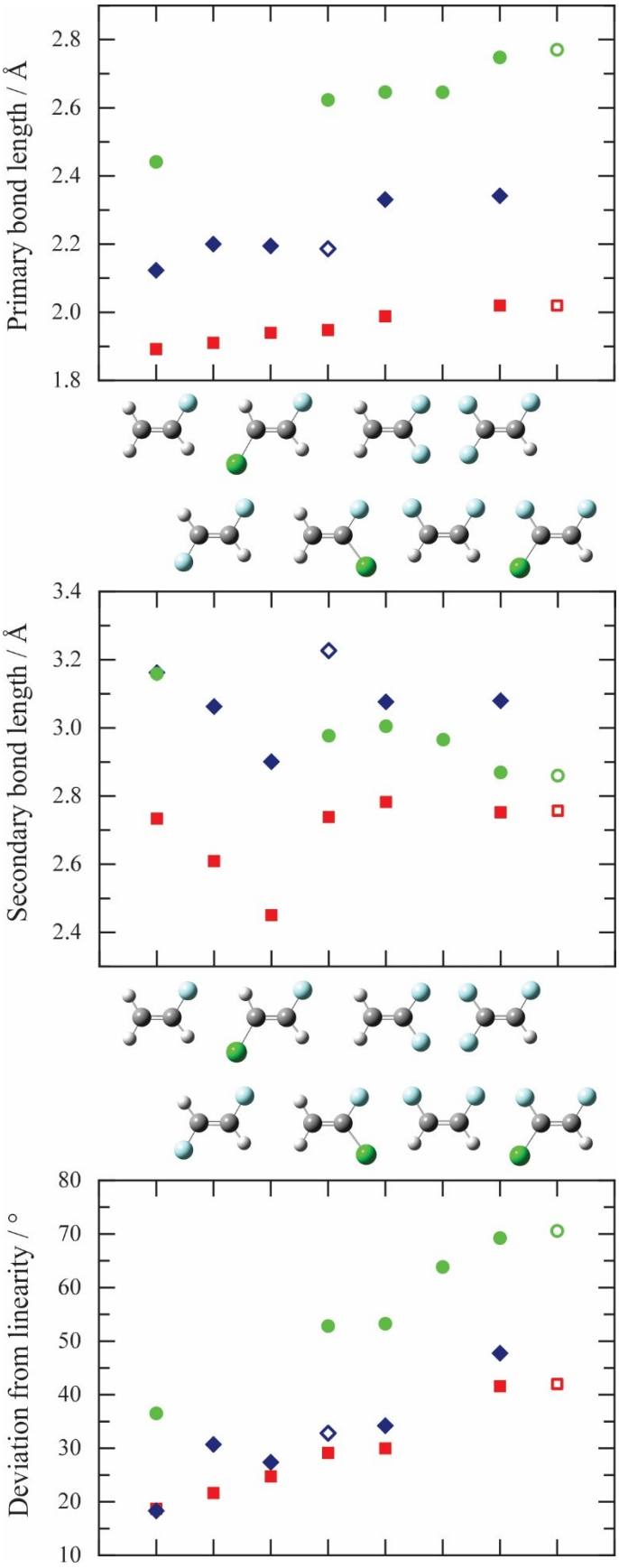

Figure 4. Primary bond length (top), secondary interaction bond length (middle), and hydrogen bond deviation from linearity for observed planar protic acid-haloethylene heterodimers with a fluorine atom hydrogen bond acceptor. The haloethylene subunits are arranged from left to right in order of increasing hydrogen bond length for the HF complex, and depicted pictorially between the panels. Red squares represent HF complexes, blue diamonds are HCl, and green circles, HCCH. Open symbols represent complexes for which only preliminary results are available. Carbon atoms are dark gray in the haloethylene subunits, hydrogen atoms light gray, fluorine atoms light blue, and chlorine atoms, green. For the vinyl fluoride species, the symbols for HCl and HCCH overlap in the middle panel, and HF and HCl overlap in the bottom.

Figure 5. Total SAPT interaction energy (top) and exchange repulsion (bottom), as a percentage of total stabilization energy, for all observed protic acid-haloethylene heterodimers. The haloethylene subunits are arranged as in Fig. 4 followed by three complexes with a chlorine atom hydrogen bond acceptor, and are depicted pictorially between the panels. Red squares represent HF complexes, blue diamonds are HCl, and green circles, HCCH. Carbon atoms are dark gray in the haloethylene monomers, hydrogen atoms light gray, fluorine atoms light blue, and chlorine atoms, green. For the 1,1,2-trifluoroethylene, the symbols for HCl and HCCH overlap in the top panel; and HF and HCCH overlap in the bottom for vinyl fluoride.

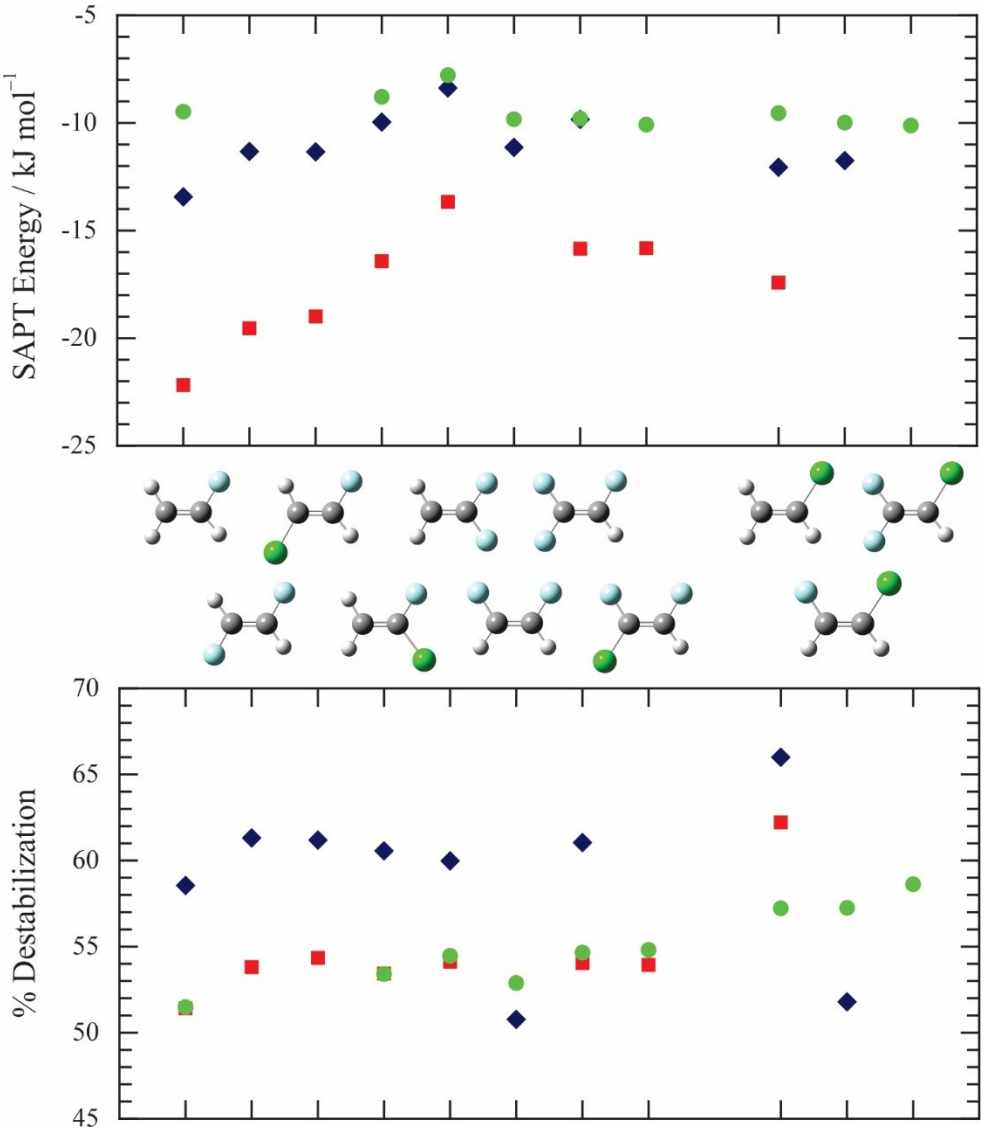

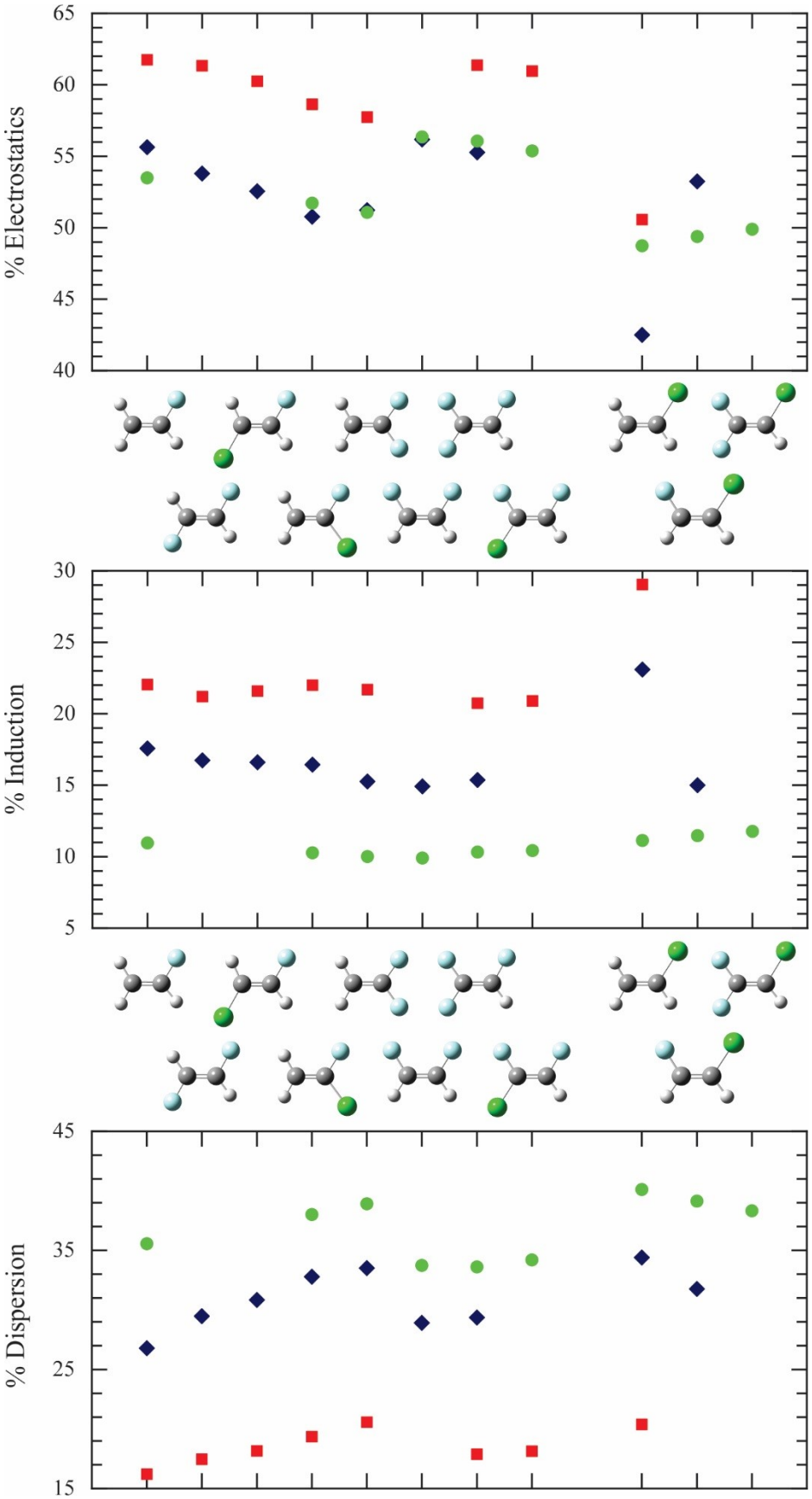

Figure 6. Contributions to SAPT binding energy from electrostatics (top), induction (middle), and dispersion (bottom), each as a percentage of total stabilization energy, for all observed protic acid-haloethylene heterodimers. The haloethylene subunits are arranged as in Fig. 4 followed by three complexes with a chlorine atom hydrogen bond acceptor, and are depicted pictorially between the panels. Red squares represent

HF complexes, blue diamonds are HCl, and green circles, HCCH. Carbon atoms are dark gray in the haloethylene subunits, hydrogen atoms light gray, fluorine atoms light blue, and chlorine atoms, green.

TOC Graphic